Cancer Science
The official journal of the Japanese Cancer Association JCA

Dietary supplementation with branched-chain amino acids suppresses diethylnitrosamine-induced liver tumorigenesis in obese and diabetic C57BL/KsJ-*db/db* mice

Junpei Iwasa,[1] Masahito Shimizu,[1,3] Makoto Shiraki,[1] Yohei Shirakami,[1] Hiroyasu Sakai,[1] Yoichi Terakura,[1] Koji Takai,[1] Hisashi Tsurumi,[1] Takuji Tanaka[2] and Hisataka Moriwaki[1]

[1]Department of Medicine, Gifu University Graduate School of Medicine, Gifu; [2]Department of Oncologic Pathology, Kanazawa Medical University, Ishikawa, Japan

(Received August 31, 2009/Revised October 5, 2009/Accepted October 6, 2009/Online publication November 9, 2009)

Obesity and related metabolic abnormalities, including insulin resistance, are risk factors for hepatocellular carcinoma in non-alcoholic steatohepatitis as well as in chronic viral hepatitis. Branched-chain amino acids (BCAA), which improve insulin resistance, inhibited obesity-related colon carcinogenesis in a rodent model, and also reduced the incidence of hepatocellular carcinoma in obese patients with liver cirrhosis. In the present study, we determined the effects of BCAA on the development of diethylnitrosamine (DEN)-induced liver tumorigenesis in obese C57BL/KsJ-*db/db* (*db/db*) mice with diabetes mellitus. Male *db/db* mice were given tap water containing 40 ppm DEN for an initial 2 weeks and thereafter they received a basal diet containing 3.0% of BCAA or casein, which served as a nitrogen content-matched control of BCAA, throughout the experiment. Supplementation with BCAA significantly reduced the total number of foci of cellular alteration, a premalignant lesion of the liver, and the expression of insulin-like growth factor (IGF)-1, IGF-2, and IGF-1 receptor in the liver when compared to the casein supplementation. BCAA supplementation for 34 weeks also significantly inhibited both the development of hepatocellular neoplasms and the proliferation of hepatocytes in comparison to the basal diet or casein-fed groups. Supplementation with BCAA improved liver steatosis and fibrosis and inhibited the expression of α-smooth muscle actin in the DEN-treated *db/db* mice. The serum levels of glucose and leptin decreased by dietary BCAA, whereas the value of the quantitative insulin sensitivity check index increased by this agent, indicating the improvement of insulin resistance and hyperleptinemia. In conclusion, oral BCAA supplementation improves insulin resistance and prevents the development of liver tumorigenesis in obese and diabetic mice. (*Cancer Sci* 2010; 101: 460–467)

Hepatocellular carcinoma is a major health problem worldwide. The development of HCC is frequently associated with chronic inflammation of the liver induced by a persistent infection with the hepatitis B virus or hepatitis C virus.[1] The risk of HCC is also elevated in those with metabolic syndrome, also called insulin resistance syndrome, which is commonly associated with obesity and impaired glucose tolerance.[1–4] Non-alcoholic fatty liver disease is known to be a hepatic manifestation of the metabolic syndrome. Diabetes mellitus, a condition associated with hyperinsulinemia, has been proposed as a risk factor for both chronic liver disease and HCC through the development of NASH, which is observed in a subset of patients with non-alcoholic fatty liver disease and involves inflammation, cell damage, and/or fibrosis in the liver.[5–7] In 1998, Day and James proposed, in their "two hit theory," that insulin resistance is regarded as a critical factor in the etiology of NASH.[8]

C57BL/KsJ-*db/db* (*db/db*) mice are a genetically altered animal model with phenotypes of obesity and diabetes mellitus. A functional defect in the long-form leptin receptor, which plays a significant role in the regulation of food intake and the control of body weight, leads to hyperleptinemia in these mice.[9] Because of such obesity, hyperinsulinemia, and hyperleptinemia, the *db/db* mice represent a suitable animal model that uniquely mimics the metabolic syndrome in humans.[10] It is also reported that the *db/db* mice are susceptible to chemically induced carcinogenesis in certain tissues. For instance, the *db/db* mice are sensitive to AOM-induced colon carcinogenesis; putative precursor lesions for colorectal cancer are greatly enhanced in *db/db* mice compared to *db/+* or +/+ mice.[11] With respect to the liver, feeding *db/db* mice with a methionine and choline-deficient diet developed accelerated hepatic inflammation and fibrosis, very similar to those seen in human NASH.[12]

An improvement of insulin resistance by nutritional or pharmaceutical intervention might therefore be an effective and attractive strategy to inhibit the obesity-related carcinogenesis, as already reported experimentally for the colon.[13] Candidate modalities include dietary supplementation with BCAA (leucine, isoleucine, and valine) because BCAA prevents progressive hepatic failure and improves the event-free survival in patients with chronic liver diseases, at least in part, by improving insulin resistance.[14–16] In addition, BCAA supplementation has been shown to prevent obesity-related colon carcinogenesis initiated with AOM[17] and, furthermore, to reduce the risk of HCC in obese patients with chronic viral liver disease.[18] In an obesity-related colon cancer model, the effects of BCAA in inhibiting the development of colonic premalignancies might be associated with improvement of insulin resistance.[17] However, whether BCAA prevents obesity-related liver carcinogenesis, and the precise mechanisms of that prevention, have not been explored.

In the present study, we examined the effects of BCAA supplementation on the development of HCC, liver cell adenoma, and FCA in obese and diabetic *db/db* mice initiated with DEN by focusing on the improvement of insulin resistance, liver steatosis, and fibrosis. We also examined whether BCAA supplementation in the diet alters the expression of IGF-1, IGF-2, and IGF-1R in the liver of DEN-treated *db/db* mice. The IGF/IGF-1R axis is closely associated with the development of HCC and might be regarded as a critical target for both HCC treatment and chemoprevention.[19,20]

[3]To whom correspondence should be addressed. E-mail: shimim-gif@umin.ac.jp

doi: 10.1111/j.1349-7006.2009.01402.x

Materials and Methods

Animals, chemicals, and diets. Four-week-old male *db/db* mice were obtained from Japan SLC (Shizuoka, Japan). All mice received humane care and were maintained at Gifu University Life Science Research Center (Gifu, Japan), according to the Institutional Animal Care Guidelines. DEN was purchased from Sigma Chemical Co. (St. Louis, MO, USA). BCAA and casein were obtained from Ajinomoto Co. (Tokyo, Japan). The BCAA composition (2:1:1.2 = leucine:isoleucine:valine) was set at the clinical dosage that is used for the treatment of decompensated liver cirrhosis in Japan.[16,18] The basal diet, CRF-1 (Oriental Yeast Co., Tokyo, Japan), contained 22.4 g of protein (1.65 g leucine, 0.83 g isoleucine, and 1.03 g valine) per 100 g of total volume.

Experimental procedure. The experimental protocol was approved by the Institutional Committee of Animal Experiments of Gifu University. At 5 weeks of age, a total of 41 *db/db* mice were divided into three groups. All the mice in Group 1 (n = 11), Group 2 (n = 15), and Group 3 (n = 15) were given tap water containing 40 ppm DEN for the initial 2 weeks. After treatment with DEN, Group 3 was given the CRF-1 supplemented with 3.0% BCAA (w/w) through to the end of experiment, whereas mice in Group 2 were given the basal diet supplemented with 3.0% casein (w/w) and served as a nitrogen content-matched control for the BCAA-treated group. Group 1 was given the CRF-1 diet throughout the experiment. In order to examine the effect of BCAA on the development of FCA in early phase, four mice each in groups 2 and 3 were starved for 6 h and killed by CO_2 asphyxiation at 23 weeks of age (after 16 weeks supplementation with BCAA or casein). At 41 weeks of age (after 34 weeks supplementation with the experimental diet), all remaining animals (total 33 mice) were killed to determine the development of HCC, liver cell adenoma, and FCA.

Histopathology and immunohistochemical analyses for α-SMA and PCNA. After the mice were killed, the livers were immediately removed and macroscopically inspected for the presence of neoplasms. Maximum sagittal sections of each lobe (six lobes) were used for histological examination. The tissue specimens were fixed in 10% buffered formaldehyde then embedded in paraffin. Serial sections (3–4 μm thick) were cut from the tissue blocks and stained with H&E for histopathology or Azan stain to observe liver fibrosis. The liver neoplasms (HCC and liver cell adenoma) and FCA were diagnosed according to criteria described previously.[21] The multiplicity of FCA was assessed on the per area basis (per cm^2).

Immunohistochemistry of α-SMA, an indicator of HSC activation, was carried out using a primary anti-α-SMA antibody (Dako, Glostrup, Denmark).[22] Immunohistochemistry of PCNA, a G_1-to-S phase marker, was carried out to estimate the cell proliferative activity of the hepatocyte using a primary anti-PCNA antibody (Santa Cruz Biotechnology, Santa Cruz, CA, USA).[23] PCNA-positive nuclei in the hepatocytes were counted and expressed as the percentage of the total number of hepatocyte nuclei. The PCNA-labeling index (%) was determined by counting at least 500 hepatocytes in each section (total of 3000 hepatocytes per mouse).

Clinical chemistry. After the mice were killed, blood samples were collected from inferior vena cava to determine the serum concentrations of ALT, glucose, insulin, leptin, and BCAA. The levels of serum glucose, insulin, and BCAA were assayed as described previously.[24,25] The serum leptin level was determined by ELISA (R&D Systems, Minneapolis, MN, USA) according to the manufacturer's protocol.[17] The serum ALT activity was measured with a standard clinical automatic analyzer (type 726; Hitachi, Tokyo, Japan). Insulin resistance was estimated by QUICKI as follows: $QUICKI = 1/[\log(I_0) + \log(G_0)]$, where I_0 is the fasting insulin and G_0 is the fasting glucose, which correlates with the glucose clamp method.[26]

Hepatic lipid analysis. To visualize intrahepatic lipids, Sudan III stain was carried out with frozen sections using the standard procedure. The hepatic lipids were also extracted from the frozen livers. Approximately 200 mg of liver was homogenized and the lipids were then extracted using chloroform:methanol (2:1 v/v) solution, as described by Folch.[27] The levels of triglyceride in the liver were measured using the triglyceride E-test kit (Wako Pure Chemical Co., Osaka, Japan) according to the manufacturer's protocol.

Hepatic hydroxyproline analysis. Hepatic hydroxyproline content was quantified colorimetrically in duplicate samples from approximately 200 mg wet-weight of liver tissue, as previously described.[22] The hydroxyproline contents were expressed as μmol/g wet liver.

Protein extraction and Western blot analysis. Equivalent amounts of protein lysates (30 μg/lane) from the liver of experimental mice were subjected to a Western blot analysis of α-SMA (Dako), as described previously.[22,23] An antibody to GAPDH (Chemicon International, Temecula, CA, USA) served as a loading control. The intensities of the blots were quantified with NIH image software version 1.62.

RNA extraction and quantitative real-time RT-PCR analysis. A quantitative real-time RT-PCR analysis was carried out as described previously.[28] Total RNA was isolated from the liver of the mice using the RNAqueous-4PCR kit (Ambion Applied Biosystems, Austin, TX, USA). The cDNA was synthesized from 0.2 μg total RNA using the SuperScript III First-Strand Synthesis System (Invitrogen, Carlsbad, CA, USA). The primers used for the amplification of *IGF-1, IGF-2*, and *IGF-1R* specific genes were as follows: *IGF-1* forward, 5′-CTGGACCAGAGACCCTTTGC-3′ and reverse, 5′-GGACGGGGACTTCTGAGTCTT-3′; *IGF-2* forward, 5′-GTGCTGCATCGCTGCTTAC-3′ and reverse, 5′-ACGTCCCTCTCGGACTTGG-3′; and *IGF-1R* forward, 5′-GTGGGGGCTCGTGTTTCTC-3′ and reverse, 5′-GATCACCGTGCAGTTTTCCA-3′. Real-time PCR was done in a LightCycler (Roche Diagnostics Co., Indianapolis, IN, USA) with SYBR Premix Ex Taq (TaKaRa Bio, Shiga, Japan). The expression levels of the *IGF-1, IGF-2*, and *IGF-1R* genes were normalized to the β-*actin* gene expression level.[28]

Statistical analysis. The results are presented as the mean ± SD, and they were analyzed using the GraphPad Instat software program version 3.05 (GraphPad Software, San Diego, CA, USA) for Macintosh. Differences among the groups were analyzed by either one-way ANOVA or, as required, by two-way ANOVA. When ANOVA showed a statistically significant effect ($P < 0.05$), comparisons of each experimental group with the control group were then made using Dunnett's test, which corrects for multiple comparisons. The differences were considered to be significant when the two-sided P value was <0.05.

Results

General observations. As shown in Table 1, there were no significant differences in the body, liver, kidney, or fat (white adipose tissue of the periorchis and retroperitoneum) weights among the groups at the end of the study. Male *db/db* mice well-tolerated the treatment with DEN together with casein or BCAA. The body weight gains did not differ significantly among the groups during the experiment (data not shown). A histopathological examination suggested the absence of toxicity of BCAA in important organs, including liver, kidney, and spleen (data not shown). In addition, no clinical signs indicating the toxicity of BCAA were observed in the mice during the experiment.

Incidence and multiplicity of DEN-induced liver neoplasms and FCA in *db/db* mice. Macroscopically, nodular lesions (Fig. 1a) were observed in the livers of experimental mice at the termination of the study (41 weeks of age). Histopathologically, these lesions were liver cell adenoma (Fig. 1b) or HCC (Fig. 1c).

Table 1. Body, liver, kidney, spleen, and fat weights of the experimental mice

Group no.	Diet	No. of mice	Weight (g) (mean ± SD)			
			Body	Liver	Kidney	Fat†
1	CRF-1	11	73.0 ± 9.2	4.4 ± 0.9	0.9 ± 1.0	7.8 ± 2.2
2	Casein	11	66.0 ± 12.0	3.8 ± 1.2	0.6 ± 0.2	5.4 ± 1.0
3	BCAA	11	68.2 ± 12.4	3.4 ± 1.3	0.6 ± 0.1	6.2 ± 1.4

†White adipose tissue of the periorchis and retroperitoneum.

FCA (Fig. 1d) also developed in the liver of experimental mice. Simultaneously, we put supplemental groups to support that *db/db* mice are actually susceptible to DEN-induced liver tumorigenesis (data not shown; see Supporting Information Table S1) and found no neoplasms in C57B6 or C57BL/KsJ-+/+ mice, genetic controls for *db/db* mice, regardless of DEN treatment. No tumors developed in the CRF-1-fed and DEN-untreated *db/db* mice.

Effects of BCAA supplementation on DEN-induced liver tumor igenesis in *db/db* mice. The incidence and multiplicity of liver neoplasms (adenoma plus HCC) and FCA at 41 weeks of age are summarized in Table 2. Compared with the CRF-1-fed mice (Group 1), dietary supplementation with BCAA (Group 3) significantly inhibited the incidence ($P < 0.05$) of adenoma. BCAA supplementation also reduced the incidence ($P < 0.05$) and multiplicity of adenoma ($P < 0.01$) compared to the casein-supplementation mice (Group 2). HCC was developed in the CRF-1-fed (9%) and casein-supplementation mice (27%), but not in the mice supplemented with BCAA (0%), and the multiplicity of total liver neoplasms was significantly inhibited by supplementation with BCAA when compared to CRF-1-fed ($P < 0.05$) or Casein-supplementation mice ($P < 0.01$), respectively. The number of FCA, which were developed in all experimental mice, was also significantly decreased by supplementation with BCAA when compared to CRF-1-fed ($P < 0.05$) or casein-supplementation mice ($P < 0.001$), respectively.

Effects of BCAA supplementation on the expression levels of *IGF-1*, *IGF-2*, and *IGF-1R* mRNAs in the liver of DEN-treated *db/db* mice. When the mice were killed at 23 weeks of age, the development of FCA was also significantly inhibited by dietary supplementation with BCAA compared with casein-supplemented mice ($P < 0.01$) (Fig. 2a). In addition, semiquantitative RT-PCR analyses showed that there was a significant decrease in the expression level of *IGF-1* ($P < 0.05$), *IGF-2* ($P < 0.05$), and *IGF-1R* mRNAs ($P < 0.05$) in the livers of the mice supplemented with BCAA when compared to that of the livers in casein-supplemented mice (Figs 2b–d). These findings suggest that BCAA supplementation prevents the development of FCA, at least in part, by inhibiting the expression of the IGF/IGF-1R axis.

Effects of BCAA supplementation on serum levels of BCAA, ALT, and leptin in DEN-treated *db/db* mice. BCAA supplementation caused a significant increase in the serum levels of BCAA compared to the CRF-1-fed ($P < 0.05$) and casein-supplemented mice ($P < 0.05$) (Fig. 3a). These findings suggest that supplementation with 3.0% BCAA is sufficient to raise the serum concentration of BCAA. The serum ALT levels markedly increased in the *db/db* mice when compared to the genetic control mice (data not shown; see Supporting Information Table S1). However, BCAA supplementation significantly decreased this value in comparison to the CRF-1-fed ($P < 0.01$) and casein-supplemented mice ($P < 0.001$) (Fig. 3b), thus indicating an improvement of liver damage. In addition, the mice supplemented with BCAA showed a decrease in the serum levels of leptin compared with the CRF-1-fed ($P < 0.001$) and casein-supplemented mice ($P < 0.001$) (Fig. 3c).

Effects of BCAA supplementation on the hepatic steatosis in DEN-treated *db/db* mice. Examination of Sudan III stained sections revealed that there was a marked macrovesicular steatosis in the DEN-treated *db/db* mice, which were fed CRF-1 or casein, but BCAA supplementation significantly improved the accumulation of the lipid in the liver (Fig. 4a). The histological findings were consistent with the results of the measurement of liver triglyceride contents; the levels of triglyceride in the liver of DEN-treated *db/db* mice were significantly decreased by the supplementation with BCAA compared to those in the CRF-1-fed ($P < 0.001$) and casein-supplementation groups ($P < 0.01$) (Fig. 4b).

Effects of BCAA supplementation on liver fibrosis in DEN-treated *db/db* mice. As shown in Figure 5a, examination of Azan-stained sections indicated that DEN-treated *db/db* mice of CRF-1-fed and casein-supplemented groups showed the development of peri-central venous and peri-cellular fibrosis. However, supplementation with BCAA yielded an improvement in liver fibrosis (Fig. 5a). Similar findings were also observed in

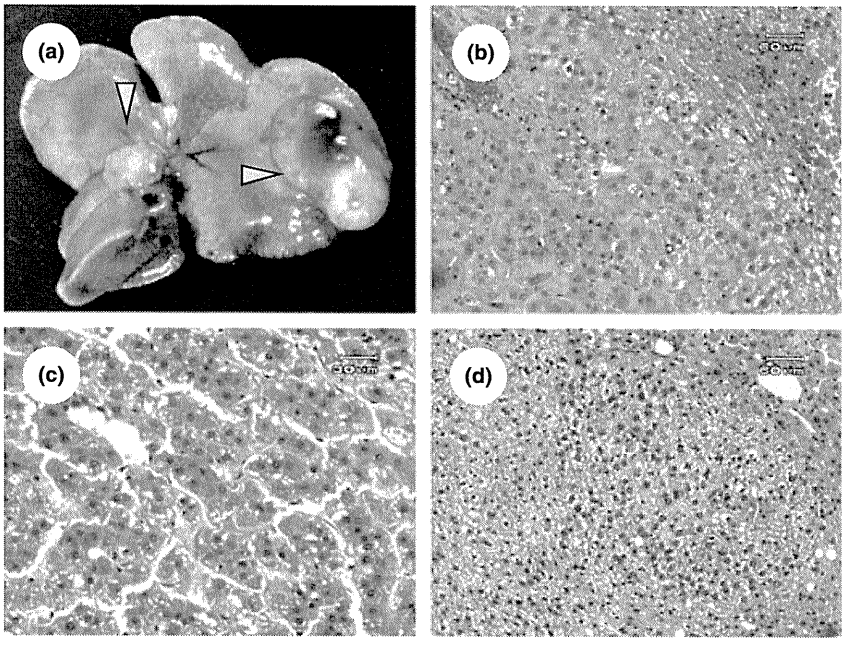

Fig. 1. Macroscopic (a) and microscopic (b–d) analyses of liver neoplasms in diethylnitrosamine-treated *db/db* mice. (a) Macroscopically, white tumors (hepatocellular carcinoma; indicated by arrowheads) were detected in the liver of diethylnitrosamine-treated C57BL/KsJ-*db/db* mice. (b–d) Paraffin-embedded sections were stained with H&E. Representative photomicrographs show adenoma (b), hepatocellular carcinoma (c), and foci of cellular alteration (d) in liver of experimental mice.

doi: 10.1111/j.1349-7006.2009.01402.x

Table 2. Incidence and multiplicity of hepatic neoplasms and foci of cellular alteration (FCA) in obese diabetic C57BL/KsJ-*db/db* mice fed basal (CRF-1), casein-supplemented, or branched-chain amino acid (BCAA)-supplemented diets

Group no.	Diet	No. of mice	Incidence (%)		Multiplicity (no. of neoplasms/mouse) (mean ± SD)			FCA (No./cm^2) (mean ± SD)
			Adenoma	HCC	Total	Adenoma	HCC	
1	CRF-1	11	7/11 (64)	1/11 (9)	1.0 ± 1.1	0.9 ± 1.1	0.1 ± 0.3	14.4 ± 4.4
2	Casein	11	8/11 (73)	3/11 (27)	1.7 ± 1.3	1.5 ± 1.1	0.3 ± 0.5	19.1 ± 5.7
3	BCAA	11	2/11 (18)*,**	0/11 (0)	0.2 ± 0.4*,***	0.2 ± 0.4***	0	9.6 ± 5.1*,****

*P < 0.05, significantly different from Group 1; **P < 0.05, significantly different from Group 2; ***P < 0.01, significantly different from Group 2; ****P < 0.001, significantly different from Group 2. HCC, hepatocellular carcinoma.

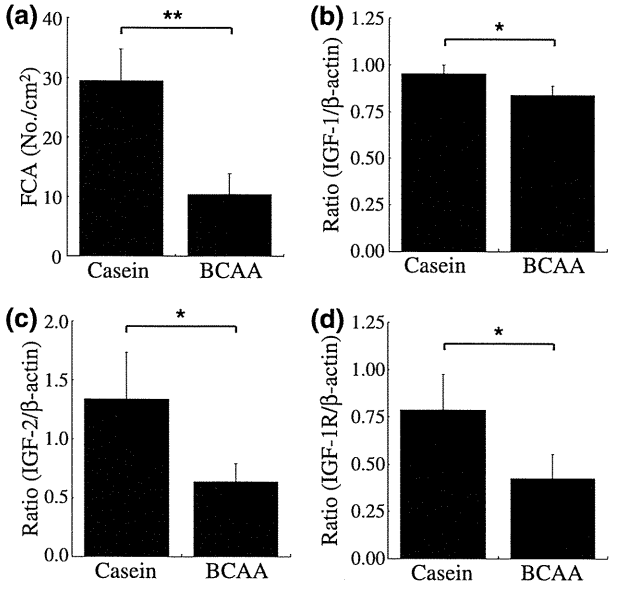

Fig. 2. Effect of branched-chain amino acid (BCAA) supplementation on the development of foci of cellular alteration (FCA) and on the expression of insulin-like growth factor (IGF)-1, IGF-2 and IGF-1 receptor (IGF-1R) mRNAs in the liver of diethylnitrosamine-treated C57BL/KsJ-*db/db* mice. Livers were excised from treated mice supplemented with casein or BCAA for 16 weeks. (a) Paraffin-embedded liver sections were stained with H&E and the total numbers of FCA were counted. Values are the means ± SD (n = 4). (b–d) Total RNA was isolated from the removed liver and the expression of *IGF-1* (b), *IGF-2* (c), and *IGF-1R* (d) genes were examined by quantitative real-time RT-PCR. The expression of each gene was normalized to β-actin expression. Each experiment was done in triplicate. *P < 0.05; **P < 0.01.

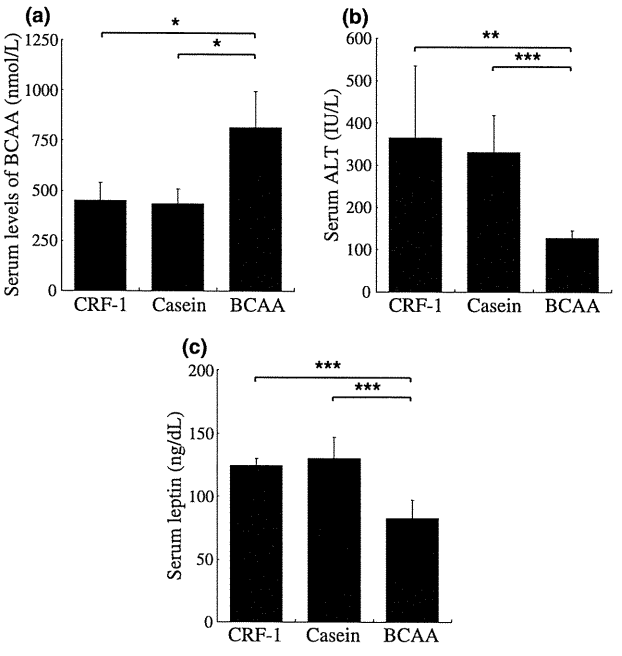

Fig. 3. Effect of branched-chain amino acid (BCAA) supplementation on the serum levels of BCAA, alanine aminotransferase (ALT), and leptin in diethylnitrosamine-treated C57BL/KsJ-*db/db* mice. After mice were killed, blood samples were collected and the serum levels of BCAA (a), ALT (b), and leptin (c) were then assayed. Values are the means ± SD (n = 8). *P < 0.05; **P < 0.01; ***P < 0.001.

the measurement of liver hydroxyproline contents, a useful marker of hepatic fibrosis;[22] when compared to CRF-1 feeding (P < 0.05) and casein supplementation (P < 0.01), BCAA supplementation caused a significant decrease in the amounts of hydroxyproline in the liver of DEN-treated *db/db* mice (Fig. 5b). In addition, both the immunohistochemical (Fig. 6a) and Western blot analyses (Fig. 6b) showed the expression levels of α-SMA in the liver to be elevated in the CRF-1-fed and casein-supplemented mice, whereas supplementation with BCAA significantly decreased the expression of this protein (P < 0.05 and P < 0.01, respectively).

Effects of BCAA supplementation on insulin resistance and serum level of glucose in DEN-treated *db/dbdb* mice. Insulin resistance plays a critical role in obesity-related HCC development.[1–4] Therefore, the effects of BCAA supplementation on the value of QUICKI and the serum levels of glucose were examined in DEN-treated *db/db* mice. As shown in Figure 7a, supplementation with BCAA caused a significant increase in the value of QUICKI compared to the CRF-1-fed (P < 0.01) and casein-supplemented mice (P < 0.01), thus indicating an improvement of insulin resistance. The serum glucose level also decreased after the supplementation with BCAA compared to CRF-1-fed (P < 0.001) and casein-supplementation (P < 0.01) (Fig. 7b).

Effects of BCAA supplementation on cell proliferative activity in liver of DEN-treated *db/db* mice. The PCNA-labeling index of non-lesional hepatocytes in DEN-treated *db/db* mice was determined based on the findings of PCNA-immunohistochemical sections (Fig. 8a). As illustrated in Figure 8b, the mean PCNA-labeling index in the BCAA-supplemented mice was significantly lower than that of the CRF-1-fed (P < 0.01) and casein-supplemented mice (P < 0.05), thus indicating that BCAA supplementation significantly inhibited cell proliferation in the liver of DEN-treated *db/db* mice.

Discussion

Recent studies have shown that obesity and diabetes mellitus are risk factors for HCC through the development of NASH.[5–7] The

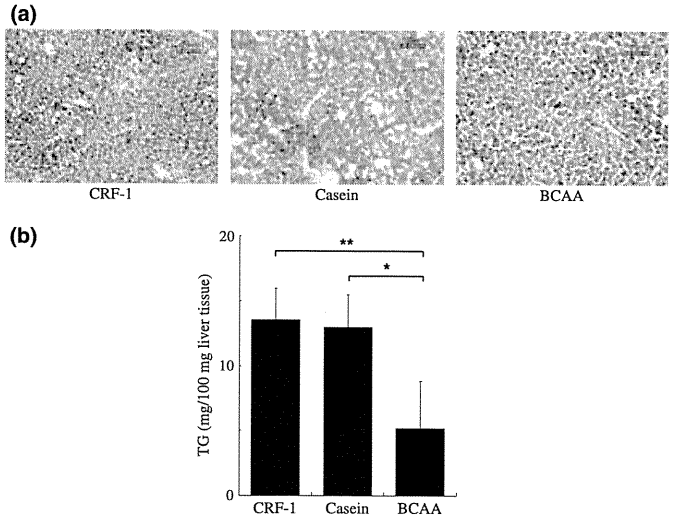

Fig. 4. Effect of branched-chain amino acid (BCAA) supplementation on hepatic steatosis in diethylnitrosamine-treated C57BL/KsJ-*db/db* mice. (a) Frozen sections of basal diet (CRF-1)-fed, casein-supplemented, or BCAA-supplemented treated mice were stained with Sudan III stain to show steatosis. (b) Hepatic lipids were extracted from the frozen livers and the levels of triglyceride were then measured. Values are the means ± SD (n = 8). *P < 0.01; **P < 0.001.

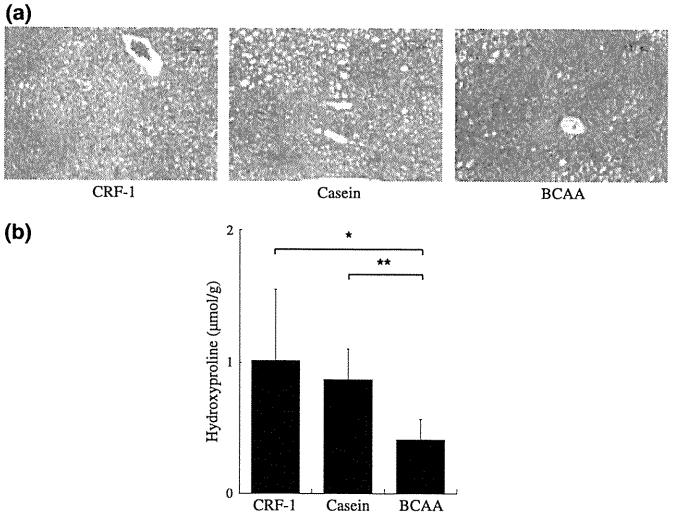

Fig. 5. Effect of branched-chain amino acid (BCAA) supplementation on hepatic fibrosis in diethylnitrosamine-treated C57BL/KsJ-*db/db* mice. (a) Paraffin-embedded sections of basal diet (CRF-1)-fed, casein-supplemented, or BCAA-supplemented treated mice were stained with Azan stain to show fibrosis. (b) Hepatic hydroxyproline contents were quantified colorimetrically. Values are the means ± SD (n = 8). *P < 0.05; **P < 0.01.

present study clearly indicated that *db/db* mice, which develop obesity and severe diabetes mellitus, easily developed steatosis-related liver neoplasms by treatment with liver carcinogen DEN (Table 2 and Fig. 1), whereas background C57B6 or C57BL/KsJ-+/+ mice did not. Furthermore, this study showed that dietary supplementation with BCAA effectively decreased the serum levels of ALT (Fig. 3b), which increase due to severe steatosis (Fig. 4a) and fibrosis (Fig. 5a), and inhibited the development of liver neoplasms (Table 2) in DEN-treated *db/db* mice. A clinical trial recently indicated that dietary supplementation with BCAA can reduce the risk of HCC in cirrhotic patients who are obese.[18] How can BCAA exert chemopreventive effects on obesity-related HCC? Presumably, the improvement of insulin resistance by BCAA (Fig. 7a) plays a critical role in this beneficial effect because, in addition to the role of insulin in glucose uptake and glycogen biosynthesis in liver and skeletal muscle, insulin has oncogenic properties on HCC cells, including the stimulation of cell growth and induction of anti-apoptotic activity.[29,30] These reports, therefore, suggest the possibility that BCAA inhibits the excessive cell proliferation in the whole liver of DEN-treated *db/db* mice (Fig. 8) by improving insulin resistance (Fig. 7a). Recent studies have also revealed that BCAA improves glucose tolerance by modulating the insulin-independent glucose uptake into skeletal muscle.[31,32] Isoleucine increased muscle glucose uptake and depressed gluconeogenesis in the liver without causing significant elevation of the plasma insulin level, thereby leading to the hypoglycemic effect in a rodent model.[33] Both improved insulin resistance and glucose tolerance by BCAA have also been indicated in clinical trials.[14,34]

In addition to the improvement of insulin resistance (Fig. 7a), the present study also indicated that dietary supplementation with BCAA significantly decreased the expression levels of *IGF-1*, *IGF-2*, and *IGF-1R* mRNAs in the liver of DEN-treated *db/db* mice (Figs 2b–d). These findings seem to be significant because abnormal activation of the IGF/IGF-1R axis, which is caused by insulin resistance, is involved in the development of HCC and, therefore, might be a critical target to prevent this malignancy.[19,20] These findings are also consistent with those of a previous report that showed BCAA supplementation decreased the serum levels of both IGF-1 and IGF-2 while also inhibiting the expression of IGF-1R on the colonic mucosa, thereby preventing the development of AOM-induced colonic neoplastic lesions in *db/db* mice.[17] This previous report,[17] together with our present findings (Fig. 2), suggest the possibility that the inhibition of IGF/IGF-1R activation is one of the critical mechanisms to suppress obesity-related tumorigenesis in specific organs, such as the colon and liver, and BCAA might be able to exert its chemopreventive effect on obesity-associated carcinogenesis by targeting this axis.

Insulin stimulates glucose uptake and triglyceride biosynthesis, which are stored in adipose tissue. The improvement of insulin resistance by BCAA, therefore, inhibits the release of free fatty acid from adipose tissue, improves hypertriglyceridemia, and thus resulted in improvement of hepatic steatosis in the present study (Fig. 4). Ectopic triglyceride accumulation in the liver is directly responsible for the development of insulin resistance.[35] In addition, several studies support the concept that hepatic steatosis promotes the development of HCC.[36] For instance, HCV core protein gene transgenic mice, a model for HCV-related hepatocarcinogenesis,[37] show marked hepatic steatosis and insulin resistance.[38,39] Hepatic steatosis is a major accelerating factor of hepatocarcinogenesis in chronic HCV infected patients.[40] In addition, a significant relationship has also been reported between steatosis and hepatic fibrosis, a potent risk factor for HCC development.[36] Therefore, the reduction of hepatic lipid accumulation might be an effective strategy for HCC chemoprevention. The improvement of hepatic steatosis (Fig. 4) and fibrosis (Fig. 5) by BCAA is thus considered to be advantageous to accomplish this objective.

There are two study limitations that might suggest additional investigations. The first is that the incidence of HCC itself was not very high in the present study (Table 2) because the duration of the experiments (41 weeks) might have been sufficient to develop adenoma but not HCC. Therefore, future study should recruit longer-term experiments to see that DEN-treated *db/db* mice develop HCC more frequently. The second is that, although our model seems to be useful to elucidate the pathogenesis underlying NASH-associated HCC, there is one difference between the liver of *db/db* mice and human NASH, as hepatic fibrosis was

doi: 10.1111/j.1349-7006.2009.01402.x

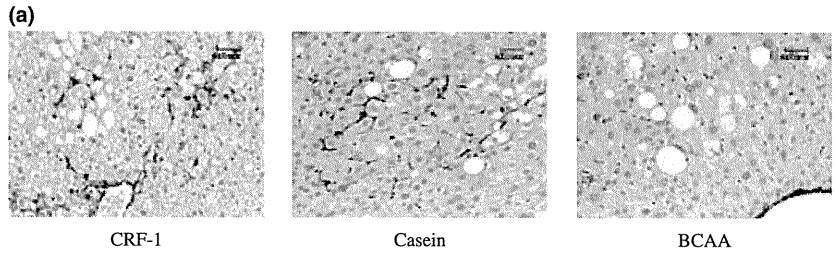

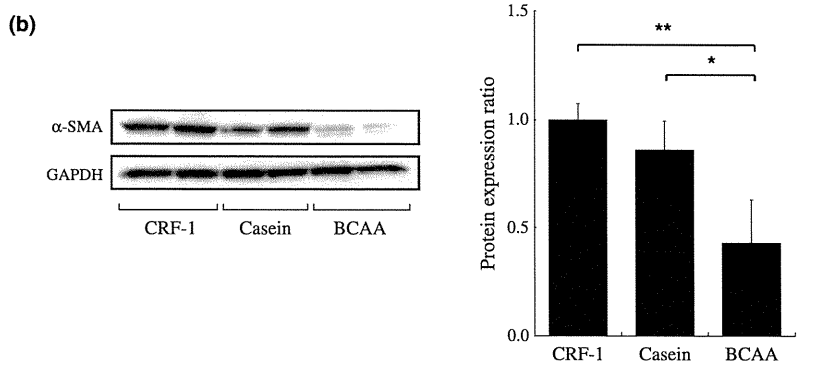

Fig. 6. Effect of branched-chain amino acid (BCAA) supplementation on the expression of α-smooth muscle actin (α-SMA) in diethylnitrosamine-treated C57BL/KsJ-*db/db* mice. (a) Immunohistochemical expression of α-SMA in the liver of basal diet (CRF-1)-fed, casein-supplemented, or BCAA-supplemented treated mice. (b) Total protein was extracted from the liver of experimental mice and the expression of α-SMA protein was examined by Western blot analysis. An antibody to GAPDH served as a loading control. Repeat Western blots gave similar results. The results obtained were quantitated by densitometry and are shown in the right-hand panels. Values are the means ± SD (n = 5). *P < 0.05; **P < 0.01.

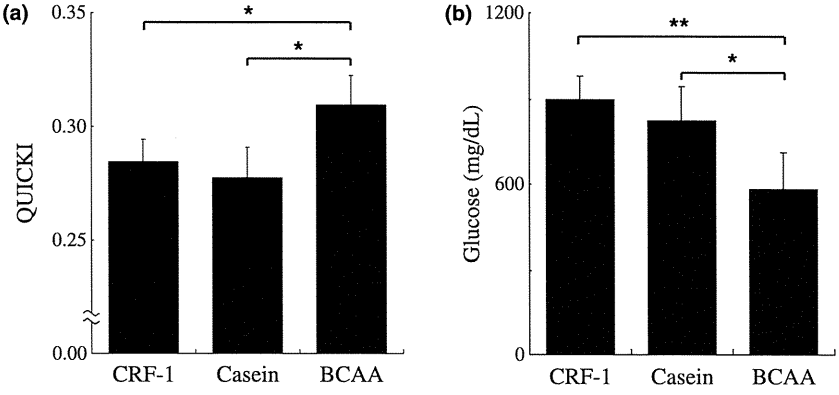

Fig. 7. Effect of branched-chain amino acid (BCAA) supplementation on insulin sensitivity and the serum level of glucose in diethylnitrosamine-treated C57BL/KsJ-*db/db* mice fed basal diet (CRF-1), or supplemented with casein or BCAA. (a) The value of the quantitative insulin sensitivity check index (QUICKI), was calculated to evaluate the insulin sensitivity. (b) The serum concentration of glucose was measured by the hexokinase method. Values are the means ± SD (n = 8). *P < 0.01; **P < 0.001.

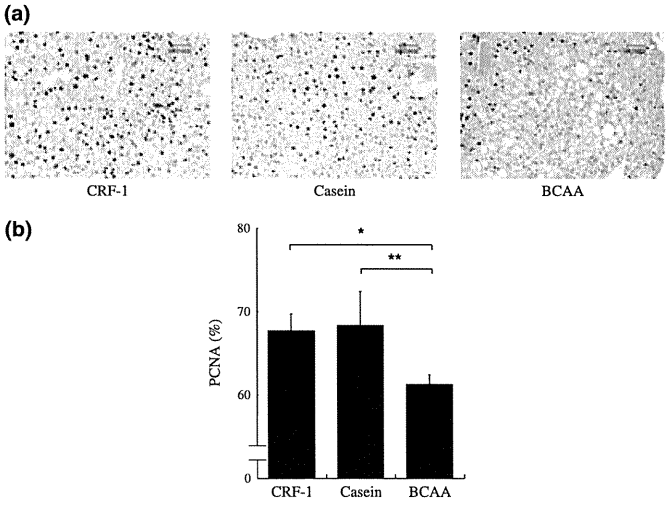

Fig. 8. Effect of branched-chain amino acid (BCAA) supplementation on hepatic cell proliferation in diethylnitrosamine-treated C57BL/KsJ-*db/db* mice. (a) Immunohistochemical expression of proliferating cell nuclear antigen (PCNA) in the liver of basal diet (CRF-1)-fed, or casein- or BCAA-supplemented treated mice. (b) PCNA-labeling index in non-lesional hepatocytes was determined by counting the PCNA-positive nuclei in the hepatocytes. *P < 0.05; **P < 0.01.

severe but did not reach liver cirrhosis at the end point of this experiment (Fig. 5a). This might be explained by a functional defect in the long-form leptin receptor because leptin exerts a pro-fibrogenic activity in the injured liver.[41,42] However, BCAA supplementation significantly decreased the serum levels of leptin (Fig. 3c), inhibited the development of liver fibrosis (Fig. 5), and suppressed the expression of α-SMA (Fig. 6), thus indicating the inhibition of HSC activation. These findings seem to be significant because activated HSCs are a major cellular source of collagen in the injured liver and thus may be a critical target for inhibiting the development of liver fibrosis.[43] Therefore, BCAA supplementation prevents the development of hepatic fibrosis, at least in part, by inhibiting the HSC activation (Fig. 6). In addition, a previous study also indicated that supplementation with BCAA effectively suppressed the hyperleptinemia in *db/db* mice with colonic carcinogenesis model.[17] These findings suggest that leptin is also one of the critical targets of BCAA in obese mice. Future studies would be important to evaluate whether BCAA could also prevent the development of liver fibrosis using a more aggressive fibrotic model, such as methionine and choline-deficient diet-fed *db/db* mice, known to be a good model of progressive NASH.[44]

Finally, it should be emphasized again that, in a recent study, BCAA supplementation in the basal diet was shown to improve insulin resistance, thereby preventing the development of colonic

premalignancies in an obesity-related colon cancer model.[17] Both obesity and insulin resistance are strongly associated with the development of not only HCC, but also colorectal cancer.[45] These previous reports, therefore, further strengthen our conclusion that the prevention of HCC by targeting the dysregulation of energy homeostasis, particularly an increased insulin resistance, might be a promising strategy for obese people who are at increased risk for developing HCC. BCAA appears to be a potentially effective and critical candidate for this purpose because it can improve insulin resistance (Fig. 7a), hepatic steatosis (Fig. 4), and fibrosis (Fig. 5) in obese and diabetic *db/db* mice.

In conclusion, BCAA might therefore represent a new effective strategy for chemoprevention against HCC, especially in obese people. Among the beneficial effects of BCAA shown in this study, the improvement of insulin resistance might play a crucial role to prevent the development of obesity-related liver tumorigenesis because the state of insulin resistance is closely associated with the activation of the IGF/IGF-1R axis, the development of hepatic steatosis and fibrosis.[5–7] In addition, a recent study revealed that BCAA supplementation also suppressed hepatic neovascularization in insulin-resistance-based hepatocarcinogenesis in obese rats.[46]

Acknowledgments

We thank Ms. Yukari Nomura for her excellent technical assistance. This work was supported in part by Grants-in-Aid from the Ministry of Education, Science, Sports and Culture of Japan (Grant No. 18790457 to M.S. and Grant No. 17015016 to H.M.).

Abbreviations

α-SMA	α-smooth muscle actin
ALT	alanine aminotransferase
AOM	azoxymethane
BCAA	branched-chain amino acids
DEN	diethylnitrosamine
FCA	foci of cellular alteration
HCC	hepatocellular carcinoma
HCV	hepatitis C virus
HSC	hepatic stellate cell
IGF	insulin-like growth factor
IGF-1R	insulin-like growth factor-1 receptor
NASH	non-alcoholic steatohepatitis
PCNA	proliferating cell nuclear antigen
QUICKI	quantitative insulin sensitivity check index

References

1 El-Serag HB, Rudolph KL. Hepatocellular carcinoma: epidemiology and molecular carcinogenesis. *Gastroenterology* 2007; **132**: 2557–76.
2 Calle EE, Rodriguez C, Walker-Thurmond K, Thun MJ. Overweight, obesity, and mortality from cancer in a prospectively studied cohort of U.S. adults. *N Engl J Med* 2003; **348**: 1625–38.
3 El-Serag HB, Hampel H, Javadi F. The association between diabetes and hepatocellular carcinoma: a systematic review of epidemiologic evidence. *Clin Gastroenterol Hepatol* 2006; **4**: 369–80.
4 El-Serag HB, Tran T, Everhart JE. Diabetes increases the risk of chronic liver disease and hepatocellular carcinoma. *Gastroenterology* 2004; **126**: 460–8.
5 Marra F, Gastaldelli A, Svegliati Baroni G, Tell G, Tiribelli C. Molecular basis and mechanisms of progression of non-alcoholic steatohepatitis. *Trends Mol Med* 2008; **14**: 72–81.
6 Saadeh S. Nonalcoholic Fatty liver disease and obesity. *Nutr Clin Pract* 2007; **22**: 1–10.
7 Smedile A, Bugianesi E. Steatosis and hepatocellular carcinoma risk. *Eur Rev Med Pharmacol Sci* 2005; **9**: 291–3.
8 Day CP, James OF. Steatohepatitis: a tale of two ''hits''? *Gastroenterology* 1998; **114**: 842–5.
9 Lee GH, Proenca R, Montez JM *et al.* Abnormal splicing of the leptin receptor in diabetic mice. *Nature* 1996; **379**: 632–5.
10 Scheen AJ, Luyckx FH. Obesity and liver disease. *Best Pract Res Clin Endocrinol Metab* 2002; **16**: 703–16.
11 Hirose Y, Hata K, Kuno T *et al.* Enhancement of development of azoxymethane-induced colonic premalignant lesions in C57BL/KsJ-db/db mice. *Carcinogenesis* 2004; **25**: 821–5.
12 Sahai A, Malladi P, Pan X *et al.* Obese and diabetic db/db mice develop marked liver fibrosis in a model of nonalcoholic steatohepatitis: role of short-form leptin receptors and osteopontin. *Am J Physiol Gastrointest Liver Physiol* 2004; **287**: G1035–43.
13 Shimizu M, Shirakami Y, Sakai H *et al.* (−)-Epigallocatechin gallate suppresses azoxymethane-induced colonic premalignant lesions in male C57BL/KsJ-db/db mice. *Cancer Prev Res* 2008; **1**: 298–304.
14 Kawaguchi T, Nagao Y, Matsuoka H, Ide T, Sata M. Branched-chain amino acid-enriched supplementation improves insulin resistance in patients with chronic liver disease. *Int J Mol Med* 2008; **22**: 105–12.
15 Marchesini G, Bianchi G, Merli M *et al.* Nutritional supplementation with branched-chain amino acids in advanced cirrhosis: a double-blind, randomized trial. *Gastroenterology* 2003; **124**: 1792–801.
16 Muto Y, Sato S, Watanabe A *et al.* Effects of oral branched-chain amino acid granules on event-free survival in patients with liver cirrhosis. *Clin Gastroenterol Hepatol* 2005; **3**: 705–13.
17 Shimizu M, Shirakami Y, Iwasa J *et al.* Supplementation with branched-chain amino acids inhibits azoxymethane-induced colonic preneoplastic lesions in male C57BL/KsJ-db/db mice. *Clin Cancer Res* 2009; **15**: 3068–75.
18 Muto Y, Sato S, Watanabe A *et al.* Overweight and obesity increase the risk for liver cancer in patients with liver cirrhosis and long-term oral supplementation with branched-chain amino acid granules inhibits liver carcinogenesis in heavier patients with liver cirrhosis. *Hepatol Res* 2006; **35**: 204–14.
19 Alexia C, Fallot G, Lasfer M, Schweizer-Groyer G, Groyer A. An evaluation of the role of insulin-like growth factors (IGF) and of type-I IGF receptor signalling in hepatocarcinogenesis and in the resistance of hepatocarcinoma cells against drug-induced apoptosis. *Biochem Pharmacol* 2004; **68**: 1003–15.
20 Shimizu M, Shirakami Y, Sakai H *et al.* EGCG inhibits activation of the insulin-like growth factor (IGF)/IGF-1 receptor axis in human hepatocellular carcinoma cells. *Cancer Lett* 2008; **262**: 10–8.
21 Frith CH, Ward JM, Turusov VS. Tumours of the liver. In: Turusor VS, Mohr U eds. *Pathology of Tumors in Laboratory Animals*. Vol 2. Lyon: IARC Scientific Publications, 1994; 223–70.
22 Yasuda Y, Shimizu M, Sakai H *et al.* (−)-Epigallocatechin gallate prevents carbon tetrachloride-induced rat hepatic fibrosis by inhibiting the expression of the PDGFR and IGF-1R. *Chem Biol Interact* 2009; **182**: 159–64.
23 Shimizu M, Hara A, Okuno M *et al.* Mechanism of retarded liver regeneration in plasminogen activator-deficient mice: impaired activation of hepatocyte growth factor after Fas-mediated massive hepatic apoptosis. *Hepatology* 2001; **33**: 569–76.
24 Shiraki M, Shimomura Y, Miwa Y *et al.* Activation of hepatic branched-chain alpha-keto acid dehydrogenase complex by tumor necrosis factor-alpha in rats. *Biochem Biophys Res Commun* 2005; **328**: 973–8.
25 Suzuki R, Kohno H, Yasui Y *et al.* Diet supplemented with citrus unshiu segment membrane suppresses chemically induced colonic preneoplastic lesions and fatty liver in male db/db mice. *Int J Cancer* 2007; **120**: 252–8.
26 Katz A, Nambi SS, Mather K *et al.* Quantitative insulin sensitivity check index: a simple, accurate method for assessing insulin sensitivity in humans. *J Clin Endocrinol Metab* 2000; **85**: 2402–10.
27 Folch J, Lees M, Sloane Stanley GH. A simple method for the isolation and purification of total lipides from animal tissues. *J Biol Chem* 1957; **226**: 497–509.
28 Tomita H, Yamada Y, Oyama T *et al.* Development of gastric tumors in Apc(Min/+) mice by the activation of the beta-catenin/Tcf signaling pathway. *Cancer Res* 2007; **67**: 4079–87.
29 Kang S, Song J, Kang H, Kim S, Lee Y, Park D. Insulin can block apoptosis by decreasing oxidative stress via phosphatidylinositol 3-kinase- and extracellular signal-regulated protein kinase-dependent signaling pathways in HepG2 cells. *Eur J Endocrinol* 2003; **148**: 147–55.
30 Tornkvist A, Parpal S, Gustavsson J, Stralfors P. Inhibition of Raf-1 kinase expression abolishes insulin stimulation of DNA synthesis in H4IIE hepatoma cells. *J Biol Chem* 1994; **269**: 13919–21.
31 Nishitani S, Takehana K. Pharmacological activities of branched-chain amino acids: augmentation of albumin synthesis in liver and improvement of glucose metabolism in skeletal muscle. *Hepatol Res* 2004; **30S**: 19–24.
32 Nishitani S, Takehana K, Fujitani S, Sonaka I. Branched-chain amino acids improve glucose metabolism in rats with liver cirrhosis. *Am J Physiol Gastrointest Liver Physiol* 2005; **288**: G1292–300.
33 Doi M, Yamaoka I, Nakayama M, Sugahara K, Yoshizawa F. Hypoglycemic effect of isoleucine involves increased muscle glucose uptake and whole body glucose oxidation and decreased hepatic gluconeogenesis. *Am J Physiol Endocrinol Metab* 2007; **292**: E1683–93.

doi: 10.1111/j.1349-7006.2009.01402.x

34 Urata Y, Okita K, Korenaga K, Uchida K, Yamasaki T, Sakaida I. The effect of supplementation with branched-chain amino acids in patients with liver cirrhosis. *Hepatol Res* 2007; **37**: 510–6.
35 Marchesini G, Brizi M, Bianchi G *et al.* Nonalcoholic fatty liver disease: a feature of the metabolic syndrome. *Diabetes* 2001; **50**: 1844–50.
36 Powell EE, Jonsson JR, Clouston AD. Steatosis: co-factor in other liver diseases. *Hepatology* 2005; **42**: 5–13.
37 Moriya K, Fujie H, Shintani Y *et al.* The core protein of hepatitis C virus induces hepatocellular carcinoma in transgenic mice. *Nat Med* 1998; **4**: 1065–7.
38 Moriya K, Yotsuyanagi H, Shintani Y *et al.* Hepatitis C virus core protein induces hepatic steatosis in transgenic mice. *J Gen Virol* 1997; **78**: 1527–31.
39 Shintani Y, Fujie H, Miyoshi H *et al.* Hepatitis C virus infection and diabetes: direct involvement of the virus in the development of insulin resistance. *Gastroenterology* 2004; **126**: 840–8.
40 Ohata K, Hamasaki K, Toriyama K *et al.* Hepatic steatosis is a risk factor for hepatocellular carcinoma in patients with chronic hepatitis C virus infection. *Cancer* 2003; **97**: 3036–43.
41 Ikejima K, Takei Y, Honda H *et al.* Leptin receptor-mediated signaling regulates hepatic fibrogenesis and remodeling of extracellular matrix in the rat. *Gastroenterology* 2002; **122**: 1399–410.
42 Leclercq IA, Farrell GC, Schriemer R, Robertson GR. Leptin is essential for the hepatic fibrogenic response to chronic liver injury. *J Hepatol* 2002; **37**: 206–13.
43 Friedman S.L. Mechanisms of hepatic fibrogenesis. *Gastroenterology* 2008; **134**: 1655–69.
44 Yamaguchi K, Yang L, McCall S *et al.* Diacylglycerol acyltranferase 1 antisense oligonucleotides reduce hepatic fibrosis in mice with nonalcoholic steatohepatitis. *Hepatology* 2008; **47**: 625–35.
45 Giovannucci E, Michaud D. The role of obesity and related metabolic disturbances in cancers of the colon, prostate, and pancreas. *Gastroenterology* 2007; **132**: 2208–25.
46 Yoshiji H, Noguchi R, Kitade M *et al.* Branched-chain amino acids suppress insulin-resistance-based hepatocarcinogenesis in obese diabetic rats. *J Gastroenterol* 2009; **44**: 483–91.

Supporting Information

Additional Supporting Information may be found in the online version of this article:

Table S1. Incidence and multiplicity of hepatic neoplasms and FCA and serum levels of ALT in db/db, +/+ and B6 mice.

Please note: Wiley-Blackwell are not responsible for the content or functionality of any supporting materials supplied by the authors. Any queries (other than missing material) should be directed to the corresponding author for the article.

Laboratory Investigation (2010) 90, 52–60

Acyclic retinoid inhibits angiogenesis by suppressing the MAPK pathway

Yusuke Komi[1,2], Yukihisa Sogabe[1], Naoto Ishibashi[3], Yasufumi Sato[4], Hisataka Moriwaki[5], Kentaro Shimokado[2] and Soichi Kojima[1]

Acyclic retinoid (ACR) is currently under clinical trial as an agent to suppress the recurrence of hepatocellular carcinoma (HCC) through its ability to induce apoptosis in premature HCC cells. ACR has an anticancer effect *in vivo* as well, although it shows weak apoptosis-inducing activity against mature HCC cells, suggesting the existence of an additional action mechanism. In this study, we investigated the antiangiogenic activity of ACR. ACR inhibited angiogenesis within chicken chorioallantoic membrane (CAM) in as similar a manner as all-*trans* retinoic acid (atRA). Although suppression of angiogenesis by atRA was partially rescued by the simultaneous addition of angiopoietin-1, suppression of angiogenesis by ACR was not rescued under the same condition at all. Conversely, although suppression of angiogenesis by ACR was partially inverted by the simultaneous addition of vascular endothelial growth factor (VEGF), suppression of angiogenesis by atRA was not affected under the same condition. These results suggested that mechanisms underlying the suppression of angiogenesis by ACR and atRA were different. ACR selectively inhibited the phosphorylation of VEGF receptor 2 (VEGFR2) and of extracellular signal-regulated kinase (ERK) without changing their protein expression levels, and inhibited endothelial cell growth, migration, and tube formation. The inhibition of the phosphorylation of ERK, endothelial growth, migration, tube formation, and angiogenesis by ACR was rescued by the overexpression of constitutively active mitogen-activated protein kinase (MAPK). Finally, ACR, but not atRA, inhibited HCC-induced angiogenesis in a xenografted CAM model. These results delineate the novel activity of ACR as an antiangiogenic through a strong inhibition of the VEGFR2 MAPK pathway.

Laboratory Investigation (2010) **90,** 52–60; doi:10.1038/labinvest.2009.110; published online 19 October 2009

KEYWORDS: ACR; HCC; MAPK pathway; phosphorylation; tumor angiogenesis; VEGF receptor

Angiogenesis has an important role in tumor growth by supplying nutrients and providing a route for metastasis.[1] Therefore, tumor angiogenesis is a good target for the treatment of solid cancers. Tumor cells induce angiogenesis by producing and releasing several angiogenic factors, such as vascular endothelial growth factor (VEGF), basic fibroblast growth factor (bFGF), and angiopoietins (Angs).[1] The VEGF/VEGF receptor (VEGFR) signaling pathway is essential for drawing endothelial cells from preexisting blood vessels and in stimulating their growth,[2] whereas the Ang/Tie2 signaling pathway is important for sustaining the interaction between endothelial and mural cells and stabilizing the vasculature.

Retinoids (vitamin A and its derivatives) are natural fat-soluble hormones, the biological effects of which are believed to be mediated, all or in part, by the modulation of target gene expression through two families of nuclear receptors: retinoic acid receptors (RARs) and retinoid X receptors (RXRs).[3] Retinoids exert antitumor activity by modifying the transactivation of $p21^{CIP1}$, interferon receptor, and signal transduction and activator of transcription.[4,5] We previously reported that all-*trans* retinoic acid (atRA) inhibits angiogenesis on chorioallantoic membrane (CAM) through disruption of vascular remodeling by inducing Ang2 expression and suppressing Ang/Tie2 signaling.[6] Acyclic retinoid (ACR)

[1]Molecular Ligand Biology Research Team, Chemical Genomics Research Group, Chemical Biology Department, RIKEN Advanced Science Institute, Saitama, Japan; [2]Department of Vascular Medicine and Geriatrics, Tokyo Medical and Dental University Graduate School, Tokyo, Japan; [3]Tokyo New Drug Research Laboratory, Pharmaceutical Division, Kowa, Tokyo, Japan; [4]Department of Vascular Biology, Institute of Development, Aging and Cancer, Tohoku University, Sendai, Japan and [5]Department of Gastroenterology, Gifu University School of Medicine, Gifu, Japan
Correspondence: Professor S Kojima, PhD, Molecular Ligand Biology Research Team, Chemical Genomics Research Group, Chemical Biology Department, RIKEN Advanced Science Institute, 2-1 Wako, Saitama 351-0198, Japan.
E-mail: skojima@postman.riken.go.jp

Received 3 February 2009; revised 20 July 2009; accepted 31 July 2009

is a synthetic retinoid and activates the RAR and RXR.[7] Oral administration of ACR for 12 months significantly reduced the incidence of post-therapeutic recurrence of hepatocellular carcinoma (HCC) compared with the placebo group.[8] In this study, ACR did not cause the typical toxic effects observed with conventional retinoids.[8] Now, ACR is under clinical trials as a chemopreventive drug against the recurrence of HCC. Nuclear receptor RXR in HCC is highly phosphorylated through the Ras-extracellular signal-regulated kinase (ERK) pathway, inactivated, and accumulates in the line as a dominant-negative receptor.[9,10] ACR inhibits the phosphorylation of RXR by inactivating the Ras-ERK pathway, recovering transactivation by retinoic acid, and induces apoptosis in human HCC cell lines.[9,10] ACR also has an anticancer effect *in vivo*.[11] However, it exerts only weak apoptosis-inducing activity against mature HCC cells *in vivo*. This result suggests an existence of an additional molecular mechanism underlying the anticancer effect of ACR. Therefore, we predicted that ACR might have antiangiogenic activity.

Herein, we found that in contrast to the antiangiogenic mechanism of atRA, ACR inhibited angiogenesis through the inhibition of the VEGF receptor mitogen-activated protein kinase (MAPK) pathway. Moreover, ACR suppressed HCC-induced angiogenesis in a xenografted CAM model. These results suggest that ACR will also be clinically useful as an antiangiogenic agent, in addition to its current usage as a chemopreventive agent.

MATERIALS AND METHODS

Reagents

Acyclic retinoid (2E,4E,6E,10E)-3,7,11,15-tetramethylhexadeca-2,4,6,10,14-pentaenoic acid) was provided by Kowa (Tokyo, Japan). AtRA was purchased from Sigma-Aldrich (St Louis, MO, USA). ACR was dissolved in ethanol and dimethyl sulfoxide (DMSO) to yield stock solutions of 10 mM and 1 M, respectively, whereas atRA was dissolved in ethanol to yield a stock solution of 17 mM.

Chicken CAM Assay

In vivo antiangiogenic activity of ACR and atRA was assessed by CAM assay as described previously.[12] In brief, fertilized Dekalb chicken eggs (Omiya Kakin, Saitama, Japan) were placed in a humidified egg incubator. After a 4.5-day incubation at 38°C, a 1% solution of methylcellulose containing ACR or atRA at various concentrations was loaded inside a silicon ring that was placed onto the surface of CAM. After a further incubation for 2 days, a fat emulsion was injected into the chorioallantois, so that the vascular networks stood out against the white background of the lipid. Antiangiogenic responses were evaluated under a stereomicroscope and photographed with a $\times 7.25$ objective. Quantitative analyses were carried out with angiogenesis-measuring software (ver.2.0; KURABO, Osaka, Japan).[12]

Matrigel Plug Assay

Matrigel (BD Biosciences, Bedford, MA, USA) was mixed with 200 units/ml heparin (Nacalai Tesque, Kyoto, Japan), with and without 50 ng/ml VEGF (Pepro Tech, Rocky Hill, NJ, USA) and 5 μM ACR in 0.1% DMSO. The matrigel mixture was injected subcutaneously into 5-week-old female C57BL/6 mice (Charles River, Yokohama, Japan). The mice were killed 7 days later. The matrigel plugs were removed and fixed in 4% paraformaldehyde for 4 h, dehydrated through a graded ethanol series, and embedded in paraffin (Nacalai Tesque). Vertical sections (5 μm) were mounted on slides and stained with hematoxylin and eosin, and observed under an inverted microscope (model DM IRB, Leica Microsystems, Wetzlar, Germany).

Cell Cultures

Human umbilical vein endothelial cells (HUVECs) and bovine aortic endothelial cells were cultured as described.[12] HepG2 cells, human HCC, were cultured in Dulbecco's modified Eagle's medium (Sigma-Aldrich) supplemented with 10% fetal calf serum.

Transfection and Luciferase Assay

Transfection into HUVECs was carried out using a combination of LipofectAMINE 2000 Plus reagent (Invitrogen) and a constitutively active MAPK kinase vector (1.5 μg each per 35-mm dish).[13]

Western Blotting Analysis

After rinsing several times with TBS (20 mM Tris–HCl, 137 mM NaCl), cells were lysed in 1% Triton X-100 in 20 mM HEPES, pH 6.8, containing Complete protease inhibitor cocktail (1 tablet per 50 ml; Roche, Indianapolis, IN, USA), 1 mM EDTA, 1 mM PMSF, and 0.5 mM Na_3VO_5, and directly subjected to western analysis using phospho-VEGFR2-specific antibodies (1:1000 dilution; Cell Signaling Technology, Danvers, MA, USA), phospho-FGFR1-specific antibodies (1:1000 dilution; Cell Signaling Technology), or phospho-ERK-specific antibodies (1:2000 dilution, Cell Signaling Technology). Cell lysates were also subjected to western analysis using antibodies to VEGFR2, FGFR1, and ERK. Immunoreactive bands of proteins were detected with ECL-Plus chemiluminescence reagents (GE Healthcare, Buckinghamshire, UK).

In Vitro Tube Formation Assay

Tube formation by HUVECs on matrigel was assessed as described previously.[14] Unpolymerized matrigel (Becton Dickinson, Bedford, MA, USA) was diluted to a final concentration of 5 mg/ml with MCDB-131 medium, aliquoted 150 μl each into 24-well plates, and allowed to polymerize for 30 min at 37°C. HUVECs were transfected with a constitutively active MAPK kinase-expressing vector. Two days later, HUVECs were seeded onto the polymerized gel at 2×10^5 cells/well; thereafter, 100 ng/ml VEGF, 1 μM, 5 μM,

and 10 μM ACR and/or atRA were added, and incubated for 6 h. *In vitro* tube formation was examined under a phase-contrast microscope and photographed with a $\times 10$ objective.

HCC-Induced Angiogenesis in a Xenografted CAM Model

Hepatocellular carcinoma-induced angiogenesis in a xenografted CAM model was assessed as previously described.[15,16] HepG2 cell suspensions with or without 5 μM ACR or atRA were delivered at 4×10^5 cells per embryo onto the top of the CAM on day 8 using a gelatin sponge, called Gelform (Pfizer, New York, NY, USA) implant. After a further 4-day incubation, a fat emulsion was injected into the chorioallantois, so that the vascular networks stood out against the white background of the lipid. Antiangiogenic responses were evaluated under a stereomicroscope and photographed with a $\times 25$.

Statistical Analysis

Data are expressed as means $\pm$ s.d. Statistical significance was assessed by one-way analysis of variance, followed by Shaffer's *t*-test.

RESULTS

Comparison Between the Effects of ACR and atRA on Blood Vessel Formation in CAM

To determine whether ACR could inhibit *in vivo* angiogenesis, we carried out CAM assay (Figure 1). The formation of intricate vascular networks, developing within control CAM

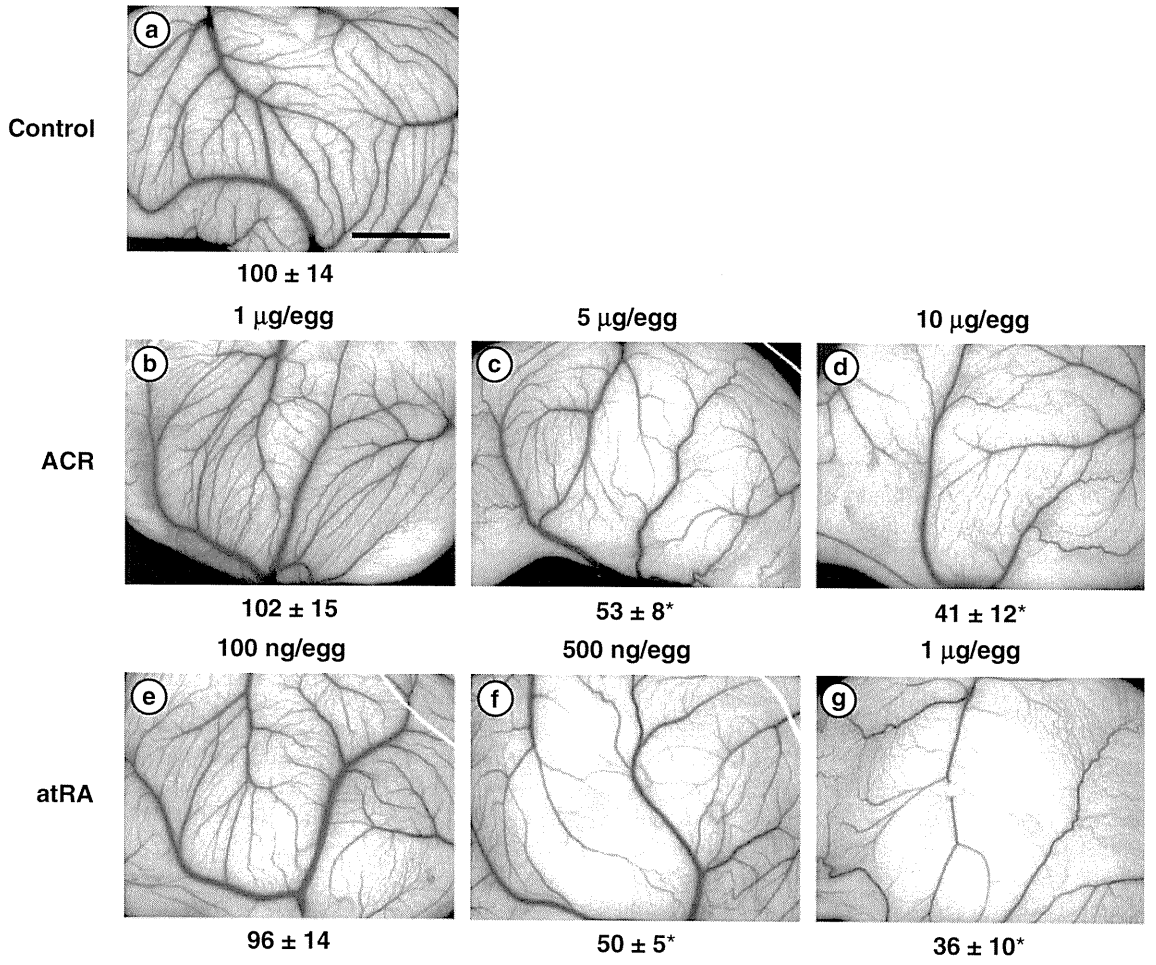

Figure 1 Suppression of *in vivo* angiogenesis in CAM by ACR and atRA. The 4.5-day-old CAMs were treated with ACR and atRA for 48 h, and then patterns of angiogenesis were photographed. Panel (**a**), vehicle (1% ethanol plus 1% DMSO); panel (**b**), 1 μg/egg ACR; panel (**c**), 5 μg/egg ACR; panel (**d**), 10 μg/egg ACR; panel (**e**), 100 ng/egg atRA; panel (**f**), 500 ng/egg atRA; panel (**g**), 1 μg/egg atRA. Scale bar, 5 mm. Total numbers of branches of blood vessels were analyzed with angiogenesis-measuring software and are shown under each panel. A total of 12 eggs (6 eggs per experiment $\times$ 2 experiments) were evaluated and representative results are shown. An asterisk indicates a significant difference ($P < 0.05$) from the control.

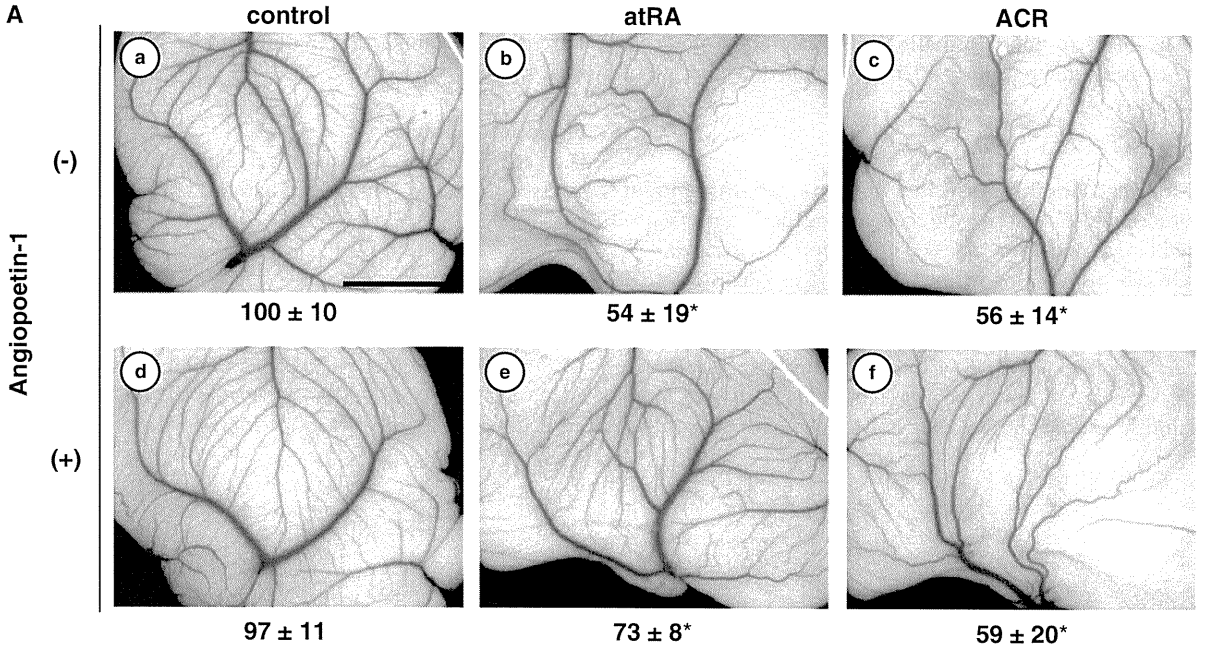

Figure 2 The antiangiogenic effect of atRA, but not ACR, was rescued by simultaneous treatment with Ang1 in CAM. (**A**) The 4.5-day-old CAMs were treated with ACR and atRA for 48 h and then patterns of angiogenesis were photographed. Panel (**a**), vehicle (1% ethanol plus 1% DMSO); panel (**b**), 500 ng/egg atRA; panel (**c**), 3 μg/egg ACR; panel (**d**), vehicle plus 300 ng/egg human recombinant Ang1; panel (**e**), 500 ng/egg atRA plus 300 ng/egg human recombinant Ang1; panel (**f**), 3 μg/egg ACR plus 300 ng/egg human recombinant Ang1. Scale bar, 5 mm. Total numbers of branches of blood vessels were analyzed with angiogenesis-measuring software and are shown under each panel. A total of 18 eggs (6 eggs per experiment × 3 experiments) were evaluated and representative results are shown. An asterisk indicates a significant difference ($P<0.05$) from the control. This result shows the representative result from three independent experiments, all of which gave similar results.

(Figure 1, panel a), was suppressed with ACR in a dose-dependent manner at concentrations of 1–10 μg/egg (0.3–3.3 mM inside the ring) (Figure 1, panels b–d) and with atRA in a dose-dependent manner at about 10 times lower concentrations of 100–1000 ng/egg (33–333 μM) (Figure 1, panels e–g). Although the inhibition of angiogenesis with atRA was partially rescued by simultaneous treatment with Ang1 at a concentration of 300 ng/egg as consistently as we reported previously[6] (Figure 2A, panel e), inhibition of angiogenesis with ACR was not rescued with Ang1 at all (Figure 2A, panel f). Furthermore, although atRA stimulated the transactivation activity of the *Ang2* promoter twofold (Supplementary Figure 1, column 2), ACR hardly showed such an activity (Supplementary Figure 1, columns 3 and 4). On the other hand, inhibition of angiogenesis with ACR, but not with atRA, was rescued by simultaneous treatment with VEGF (compare Figure 3A, panels e and f). To determine whether ACR might inhibit VEGF-induced blood vessel formation *in vivo*, we examined the effect of ACR in the matrigel plug assay (Figure 3B). Invasion of cells into gels was observed in the control matrigel that contained VEGF without ACR (panel a). When ACR was included in the matrigel at a concentration of 5 μM, the VEGF-induced invasion of cells was inhibited by about 54% (panel b).

Effect of ACR and atRA on Endothelial Cell Growth, Migration, and Tube Formation

We investigated the molecular mechanism by which ACR inhibited angiogenesis. First, we compared the effect of ACR and atRA on vascular endothelial cells. ACR (5 μM) suppressed the growth, migration, and tube formation (Figure 4A, lane 2, closed column; Figure 4B, lane 2, closed column; Figure 4C, panel b, respectively). These suppressive effects by ACR were, all or in part, rescued by overexpressing a constitutive active *MEK* gene (Figure 4A, lane 2, open column; Figure 4B, lane 2, open column; Figure 4C, panel e, respectively). Conversely, atRA did not suppress, rather it enhanced all of them (Figure 4A, lane 3, closed column; Figure 4B, lane 3, closed column; Figure 4C, panel c, respectively).

ACR Suppressed Phosphorylation of VEGFR2 and ERK

Next, we examined the effect of ACR and atRA on the phosphorylation of angiogenic growth factor receptors expressed by endothelial cells. As seen in the upper panel of Figure 5a, induction of phosphorylated 230 kD VEGFR2 after VEGF treatment was blocked to about 20% by pretreatment with 5 μM ACR for 24 h (compare lanes 4 with 5). In contrast, pretreatment with 5 μM atRA for 24 h did not block the

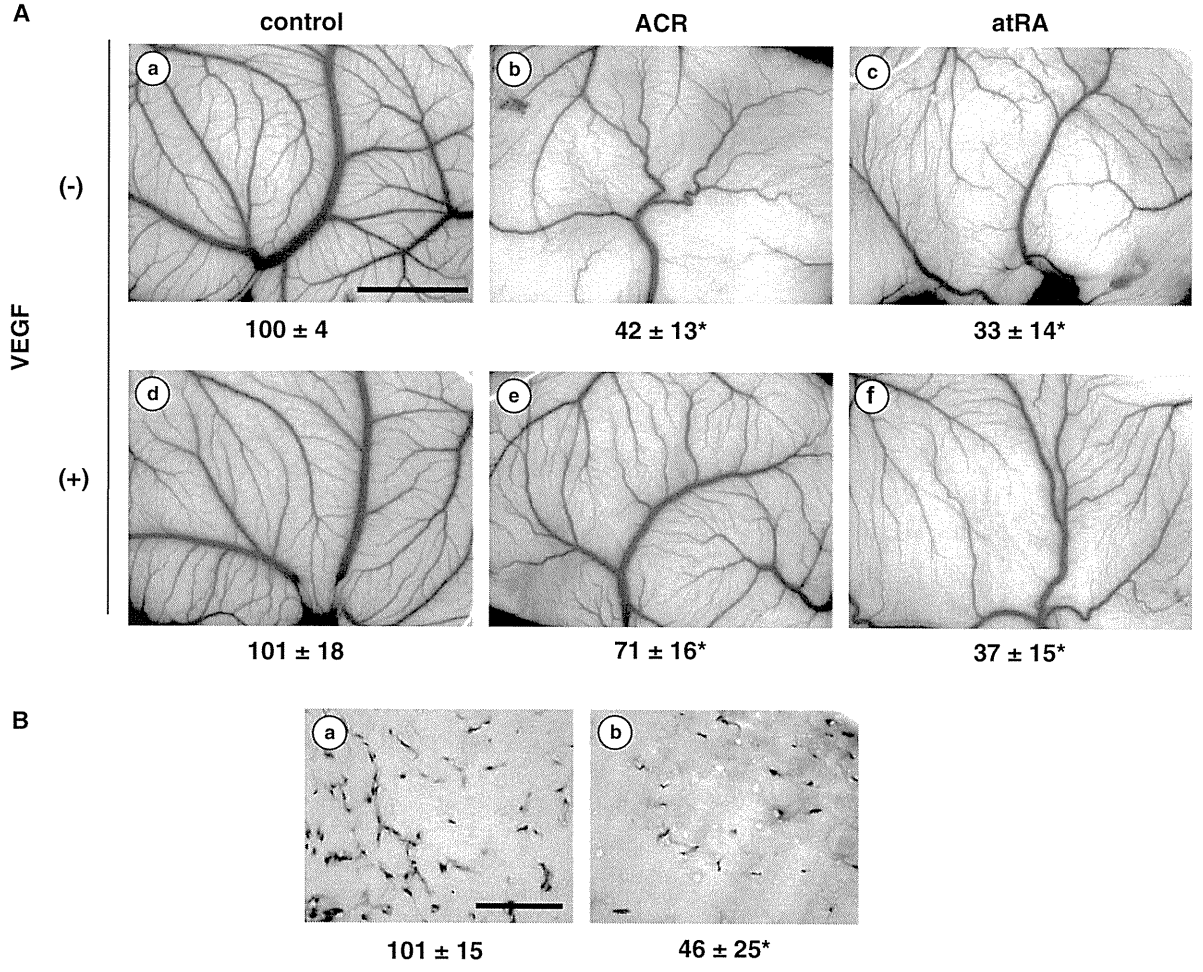

Figure 3 The antiangiogenic effect of ACR, but not of atRA, was rescued by simultaneous treatment with VEGF in CAM (**A**). The 4.5-day-old CAMs were treated with ACR and atRA for 48 h and then patterns of angiogenesis were photographed. Panel (**a**), vehicle (1% ethanol plus 1% DMSO); panel (**b**), 3 μg/egg ACR; panel (**c**), 500 ng/egg atRA; panel (**d**), vehicle plus 1 ng/egg mouse recombinant VEGF; panel (**e**), 3 μg/egg ACR plus 1 ng/egg mouse recombinant VEGF; panel (**f**) 500 ng/egg atRA plus 1 ng/egg mouse recombinant VEGF. Scale bar, 5 mm. Total numbers of branches of blood vessels were analyzed with angiogenesis-measuring software and are shown under each panel. A total of 18 eggs (6 eggs per experiment × 3 experiments) were evaluated and representative results are shown. (**B**) Matrigel plug assay: matrigel plugs containing 50 ng/ml VEGF ± 5 μM ACR were implanted into mice subcutaneously. One week later, matrigel plugs were collected and stained with hematoxylin and eosin (panels a and b). Panel **a**, VEGF alone (control); panel **b**, VEGF plus ACR. Representative data from a total of nine micrographs (3 fields × 3 mice) are presented. Scale bar, 500 μm. The number of invading cells in each micrograph was counted and the relative values are presented as percentages under each photograph. An asterisk indicates a significant difference ($P<0.05$) from the control. Panels **A** and **B** show representative results from two independent experiments, both of which gave similar results.

phosphorylation of VEGFR2 but rather increased it (compare lanes 4 with 6). Both ACR and atRA decreased the expression of VEGFR2 to about 70 and 60%, respectively, without VEGF treatment (compare lanes 1 with 2 and 3). However, this effect was not obvious in cells treated with VEGF (compare lanes 4–6). ACR did not affect the binding of VEGF to VEGFR2, nor did it affect *VEGF* mRNA levels (data not shown). On the other hand, pretreatment with ACR or atRA did not block the phosphorylation of FGFR1 but rather enhanced it (Figure 5b). Whereas ACR inhibited the phosphorylation of Ras, it did not inhibit the phosphorylation of Akt (Supplementary Figure 2). In addition, pretreatment with 5 μM ACR, but not with atRA, significantly inhibited the phosphorylation of ERK, which is induced downstream of VEGF stimuli (Figure 6a, lanes 5 and 6 in upper panel, respectively). The inhibition by ACR was inverted by the overexpression of constitutively active MAPK kinase in HUVECs (Figure 6b, lane 4 in upper panel).

Effect of ACR and atRA on HCC-Induced Angiogenesis in a Xenografted CAM Model

To confirm whether ACR and atRA have anti-HCC-induced angiogenic activity *in vivo*, we investigated the effect of ACR and atRA on HCC-induced angiogenesis in a xenografted

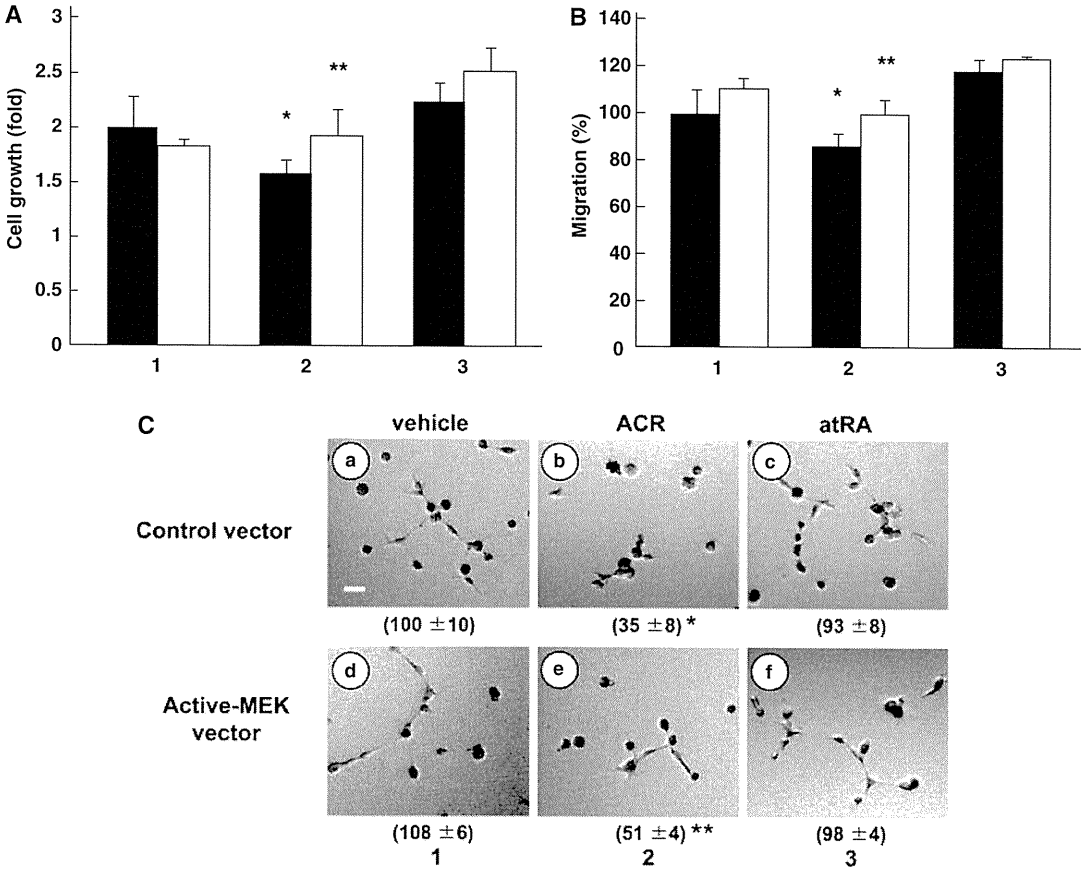

Figure 4 Effects of ACR and atRA on endothelial cell growth, migration, and tube formation. (**A**) HUVECs were transfected with a constitutively active MAPK kinase-expressing vector. After 2 days, cells (1×10^5 cells) were seeded onto 3.5-cm dishes and incubated for another 2 days. They were then incubated for 48 h in α-MEM medium containing 10% fetal calf serum, 100 ng/ml VEGF, and 5 μM ACR or atRA. Cells were counted and cell numbers are plotted as ploidy relative to values for untreated control cells at the start of incubation with ACR or atRA. Values represent means ± s.e. ($n = 2$). Lane 1, vehicle (0.1% ethanol); lane 2, ACR; lane 3, atRA. Closed columns, cells overexpressing control vector; open columns, cells overexpressing constitutively active MAPK kinase. A single asterisk indicates a significant difference ($P < 0.05$) from the control (lane 1, closed column) and double asterisks indicate a significant difference ($P < 0.05$) between samples with or without the overexpression of constitutively active MAPK kinase. (**B**) HUVECs were transfected with a constitutively active MAPK kinase-expressing vector. After 2 days, cells were wounded with a tip of pipette and incubated for 12 h in α-MEM medium containing 2.5% fetal calf serum, 100 ng/ml VEGF, and 5 μM ACR or atRA. The numbers of cells that migrated into the denuded area were counted and are plotted as percentages relative to values for untreated control cells. Values represent means ± s.e. ($n = 2$). Lane 1, vehicle (0.1% ethanol); lane 2, ACR; lane 3, atRA. Closed columns, cells overexpressing control vector; open columns, cells overexpressing constitutively active MAPK kinase. A single asterisk indicates a significant difference ($P < 0.05$) from the control (lane 1, closed column) and double asterisks indicate a significant difference ($P < 0.05$) between samples without or with the overexpression of constitutively active MAPK kinase. (**C**) HUVECs were transfected with a constitutively active MAPK kinase-expressing vector. After 2 days, cells were seeded onto polymerized matrigel at 2×10^5 cells/well. Thereafter, 100 ng/ml VEGF and 5 μM ACR or atRA were added, and incubated for 6 h. Patterns of tube formation were photographed. Scale bar, 100 μm. Panels (**a–c**), cells overexpressing control vector; panels (**d–f**), cells overexpressing constitutively active MAPK kinase. Panels (**a** and **d**), vehicle (0.1% ethanol) plus 100 ng/ml VEGF; panels (**b** and **e**), 5 μM ACR plus 100 ng/ml VEGF; panels (**c** and **f**), 5 μM atRA plus 100 ng/ml VEGF. The numbers of branches in each micrograph were counted and the relative values are presented as percentages under each photograph. A single asterisk indicates a significant difference ($P < 0.05$) from the control (panel **a** *vs* panel **b**) and double asterisks indicate a significant difference ($P < 0.05$) between samples with or without the overexpression of constitutively active MAPK kinase (panel **b** *vs* panel **e**). Panels **A–C** show representative results from two independent experiments, both of which gave similar results.

CAM model (Figure 7). Although 5 μM ACR inhibited HCC-induced angiogenesis by 37% (panel b), the same concentration of atRA did not show any inhibition at all (panel c). This result suggested that ACR, but not atRA, may prevent the recurrence of HCC in part through the inhibition of cancer angiogenesis.

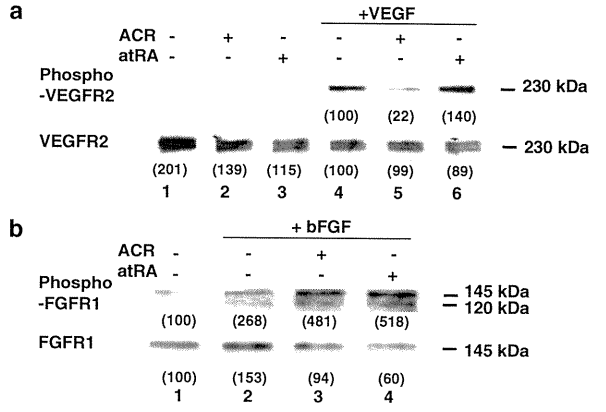

Figure 5 Effects of ACR and atRA on phosphorylation of growth factor receptors. After HUVECs had been incubated for 24 h with or without 5 μM ACR or atRA in medium containing 2.5% serum, cells were stimulated with either 100 ng/ml VEGF (panel **a**) or 50 ng/ml bFGF (panel **b**) for 5 min, and then lysed immediately. The amounts of each phosphorylated receptor (each upper bands), as well as whole amounts of each receptor (each lower bands), were assessed as described in the Materials and methods section. Panels **a** and **b** show representative results from two independent experiments, both of which gave similar results.

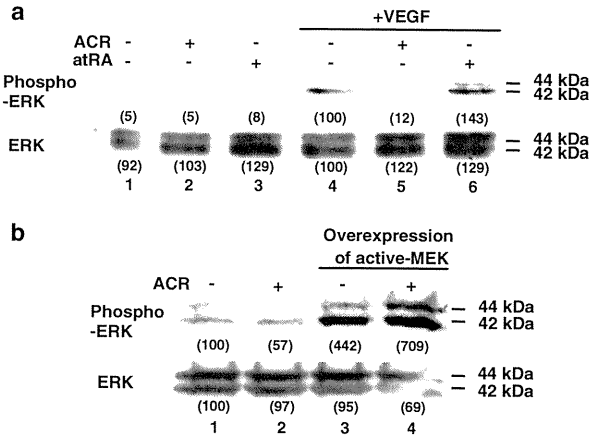

Figure 6 Effect of ACR on phosphorylation of ERK. (**a**) After HUVECs had been incubated for 24 h with or without 5 μM ACR or atRA in medium containing 2.5% serum, cells were stimulated with 100 ng/ml VEGF for 5 min and then lysed immediately. (**b**) HUVECs were transfected with a constitutively active *MEK* gene. The day after transfection, the medium was changed and cells were treated with 5 μM ACR and lysed immediately. The amounts of each phosphorylated ERK (upper bands), as well as whole amounts of ERK (lower bands), were assessed as described in the Materials and methods section.

DISCUSSION

In this paper, we have shown an antiangiogenic activity of ACR and its underlying molecular mechanism, differing from that of atRA. Although the relative antiangiogenic activity of ACR was about 10 times weaker than that of atRA at the same concentrations (Figure 1), ACR showed much stronger inhibition in endothelial cell growth, migration, and tube formation than atRA (Figure 4) because of suppression in the VEGF-MAPK pathway (Figures 5 and 6). ACR suppressed the phosphorylation of VEGFR2 (Figure 5a, lane 5). On the other hand, atRA induced the phosphorylation of VEGFR2 (Figure 5a, lane 6). This might be because of the induction of VEGF by atRA as reported previously.[17] ACR did not affect the levels of *VEGF* mRNA and the transactivation of the *VEGF* promoter (data not shown). ACR slightly inhibited the phosphorylation of VEGFR1 at 300 μM but not at all at 30 μM (Ishibashi *et al*, unpublished data). ACR (1 or 10 μM) did not inhibit other tyrosine kinases (for example, EGFR, FGFR3, FLT3, IGF1R, MET, PDGFR-α, PDGFR-β, and TRKB) (Ishibashi *et al*, unpublished data). Moreover, ACR inhibited the phosphorylation of Ras but not the phosphorylation of Akt (Supplementary Figure 2). Therefore, we speculate that ACR may selectively interfere with the phosphorylation of VEGFR2 after Ras activation, although it is not clear how ACR does this; the underlying detailed molecular mechanism(s) remain to be elucidated. ACR and atRA enhanced the phosphorylation of FGFR1 (Figure 5b, lanes 3 and 4). This result might be because of the induction of bFGF by atRA as previously reported.[18] ACR might also induce bFGF, probably through its retinoid activity.

These results suggest that suppression of the recurrence of HCC by ACR was induced in part through its antiangiogenic property by directly suppressing endothelial growth, migration, and tube formation through inhibition of the VEGFR2-MAPK axis. On the other hand, atRA inhibits angiogenesis by a disruption of vascular networks through an increased expression of Ang2 and inhibition in the Ang/Tie2 pathway.[6] Compared with atRA, ACR has 1/10–1/100 weaker 'retinoid' activities.[19] It has a 1/10 weaker action on leukemia differentiation,[20] and a 1/100 weaker carcinogenic action in transgenic mice that express the dominant-negative form of retinoic acid receptor.[21,22] On the other hand, accumulating evidence shows that ACR, but not atRA, has apoptosis-inducing activity in HCC cells, as well as in smooth muscle cells and vascular neointima.[23,24] We found that ACR acts as either a kinase inhibitor or a phosphatase stimulator and prevents hyperphosphorylation of RXR,[9] and now VEGFR2. In this context, we speculate that ACR resembles geranylgeraniol in terms of its isoprenoid-like structure, which has been implicated in the modulation of many phosphorylation/dephosphorylation signaling.[25,26]

Hepatocellular carcinoma is a major cause of cancer mortality worldwide, especially in Southeast Asia and in sub-Saharan Africa.[27] The development of HCC is frequently associated with a chronic inflammation of the liver induced by persistent infection with hepatitis B virus or hepatitis C virus. The annual incidence rises to ~20–25% in cirrhotic patients who have undergone a potentially curative removal of primary HCC in Japan; the recurrence rate at 5 years after the curative treatment may exceed 70%. This high recurrence rate is not because of local recurrence or metastasis from the original lesion, but rather from a second primary lesion.[19]

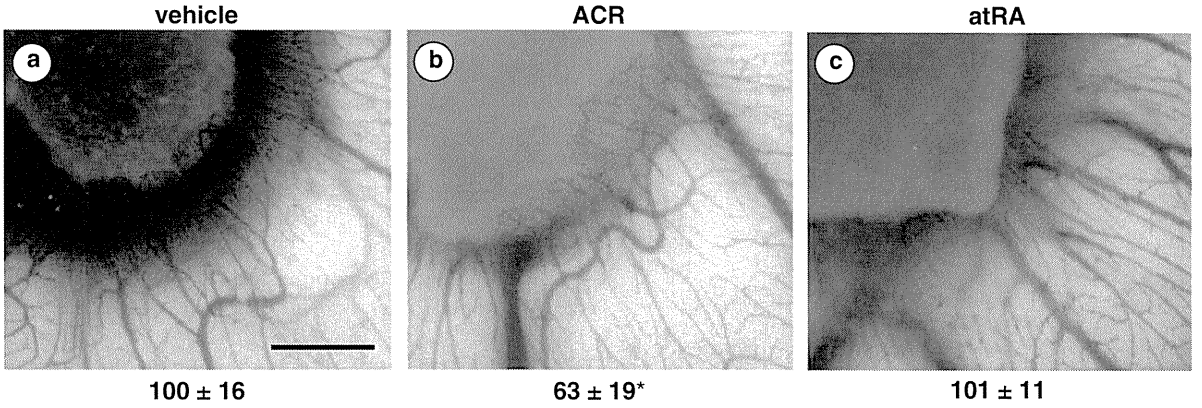

Figure 7 Effect of ACR on HCC-induced angiogenesis on CAM. HepG2 cell suspensions with or without 5 μM ACR or atRA were delivered at 4×10^5 cells per embryo onto the top of CAM on day 8 using a gelatin sponge implant. After a further 4-day incubation, a fat emulsion was injected into the chorioallantois, so that the vascular networks stood out against the white background of the lipid, and patterns of angiogenesis toward the implant were photographed. Panel (**a**), vehicle (1% EtOH); panel (**b**), 5 μM ACR; panel (**c**), 5 μM atRA. Scale bar, 1 mm. Total numbers of branches of blood vessels were counted and the relative values are presented as percentages under each photograph. An asterisk indicates a significant difference ($P<0.05$) from the control. This result shows the representative result from two independent experiments, both of which gave similar results.

In HCC tissues, RXR-α is constitutively phosphorylated by the activation of MAPK, resulting in a loss of its function and accumulation of inactive RXR-αs inside cells as dominant-negative inhibitors.[9,10] Therefore, phosphorylation of RXR-α causes a reduction in transactivation through a RAR/RXR complex.[9,28] ACR inhibits the phosphorylation of RXR-α and restores the function of RXR-α, and thereby transactivation through the RAR/RXR complex with endogenous retinoic acid. Retinoids are thought to activate the transcription of cell cycle inhibitor $p21^{CIP1}$ by RAR[29] and by apoptosis-inducer tissue transglutaminase in HCC.[19] However, 5 μM ACR hardly induces endothelial cell death (Figure 4A) and expression of $p21^{CIP1}$ mRNA levels in endothelial cells (data not shown). We found that phosphorylation of RAR/RXR was associated with the growth of endothelial cells and that ACR inhibited this phosphorylation (Supplementary Figure 3). As this phosphorylation of RAR/RXR coincided with the activation of VEGFR2 and Ras and as we had already found that RAR/RXR phosphorylation was induced by the overexpression of active MEK in cancer cells,[10] we speculate that phosphorylation of RAR/RXR would occur downstream of the VEGF/VEGFR axis in growing endothelial cells.

Acyclic retinoid suppressed both angiogenesis and HCC-induced angiogenesis in a xenografted CAM model (Figure 1, panels b–d and Figure 7, panel b, respectively). In this model, ACR did not affect the preexisting blood vessels on CAM. These results suggest that ACR did not affect the mature blood vessel and only affected neovasculature formation, including both normal angiogenesis and tumor angiogenesis. On the other hand, atRA suppressed angiogenesis but failed to suppress the tumor angiogenesis on CAM (Figures 1 and 7, panels e–g and panel c, respectively), suggesting that atRA inhibits angiogenesis in the embryonic stage, but not tumor-induced angiogenesis, and addressing the superiority of ACR as a promising antitumor angiogenesis agent. The dose of ACR used in this experiment (5 μM) is higher than the maximal blood concentration of ACR in clinical use (1 μM) (Ishibashi *et al*, unpublished data). However, we believe that liver tissue has higher doses of ACR than does the blood level because of the accumulation of ACR in the liver. These results suggest that one of the mechanisms of ACR action to prevent recurrence of HCC is its antiangiogenic activity.

Supplementary Information accompanies the paper on the Laboratory Investigation website (http://www.laboratoryinvestigation.org)

ACKNOWLEDGEMENTS

The authors thank Dr NG Ahn (University of Colorado, CO) for providing the constitutively active MAPK kinase vector. This study was supported in part by grants from the Chemical Genomics Research Project from RIKEN (to SK) and Grant-in-Aids from the Ministry of Education, Science, Sports, and Culture (17015016, HM).

DISCLOSURE/CONFLICT OF INTEREST

The authors declare no conflict of interest.

1. Mazitschek R, Giannis A. Inhibitors of angiogenesis and cancer-related receptor tyrosine kinase. Curr Opin Chem Biol 2004;8:432–441.
2. Ferrara N, Kerbel R. Angiogenesis as a therapeutic target. Nature 2005;438:967–974.
3. Chambon P. A decade of molecular biology of retinoic acid receptors. FASEB J 1996;10:940–954.
4. Obora A, Shiratori Y, Okuno M, *et al.* Synergistic induction of apoptosis by acyclic retinoid and interferon-β in human hepatocellular carcinoma cells. Hepatology 2002;36:1115–1124.
5. Altucci L, Leibowitz MD, Ogilvie KM, *et al.* RAR and RXR modulation in cancer and metabolic disease. Nat Rev Drug Discov 2007;6:793–810.
6. Suzuki Y, Komi Y, Ashino H, *et al.* Retinoic acid controls blood vessel formation by modulating endothelial and mural cell interaction via suppression of Tie2 signaling in vascular progenitor cells. Blood 2004;104:166–169.

7. Altucci L, Gronemever H. The promise of retinoids to fight against cancer. Nat Rev Cancer 2001;1:181–193.
8. Muto Y, Moriwaki H, Ninomiya M, *et al.* Prevention of second primary tumors by an acyclic retinoid, polyprenoic acid, in patients with hepatocellular carcinoma. N Engl J Med 1996;334: 1561–1568.
9. Matsushima-Nishiwaki R, Okuno M, Takano Y, *et al.* Molecular mechanism for growth suppression of human hepatocellular carcinoma cells by acyclic retinoid. Carcinogenesis 2003;24: 1353–1359.
10. Matsushima-Nishiwaki R, Okuno M, Adachi S, *et al.* Phosphorylation of retinoid X receptor α at serine 260 impairs its metabolism and function in human hepatocellular carcinoma. Cancer Res 2001;61: 7675–7682.
11. Kagawa M, Tetsuo S, Ishibashi N, *et al.* An acyclic retinoid, NIK-333, inhibits *N*-diethylnitrosamine-induced rat hepatocarcinogenesis through suppression of TGF-α expression and cell proliferation. Carcinogenesis 2004;25:979–985.
12. Komi Y, Suzuki Y, Shimamura M, *et al.* Mechanism of inhibition of tumor angiogenesis by β-hydroxyisovalerylshikonin. Cancer Sci 2009;100:269–277.
13. Mansour SJ, Matten WT, Hermann AS, *et al.* Transformation of mammalian cells by constitutively active MAP kinase kinase. Science 1994;265:966–970.
14. Komi Y, Ohno O, Suzuki Y, *et al.* Inhibition of tumor angiogenesis by targeting endothelial surface ATP synthase with sangivamycin. Jpn J Clin Oncol 2007;37:867–873.
15. Rabatti D, Nico B, Vacca A, Presta M. The gelatin sponge-chorioallantoic membrane assay. Nat Protoc 2006;1:85–91.
16. Chen MJ, Chiou PP, Lin P, *et al.* Suppression of growth and cancer-induced angiogenesis of aggressive human breast cancer cells (MDA-MB-231) on the chorioallantoic membrane of developing chicken embryos by E-peptide of pro-IGF-I. J Cell Biochem 2007;101:1316–1327.
17. Saito A, Sugawara A, Uruno A, *et al.* All-trans retinoic acid induces *in vitro* angiogenesis via retinoic acid receptor: possible involvement of paracrine effects of endogenous vascular endothelial growth factor signaling. Endocrinology 2007;148:1412–1423.
18. Gaetano C, Catalano A, Illi B, *et al.* Retinoids induce fibroblast growth factor-2 production in endothelial cells via retinoic acid receptor α activation and stimulate angiogenesis *in vitro* and *in vivo*. Circ Res 2001;88:E38–E47.
19. Kojima S, Okuno M, Matsushima-Nishiwaki R, *et al.* Acyclic retinoid in the chemoprevention of hepatocellular carcinoma (Review). Int J Oncol 2004;24:797–805.
20. Tsurumi H, Tojo A, Takahashi T, *et al.* Differentiation induction of human promyelocytic leukemia cells by acyclic retinoid (polyprenoic acid). Int J Hematol 1993;59:9–15.
21. Sakabe T, Tsuchiya H, Endo M, *et al.* An antioxidant effect by acyclic retinoid suppresses liver tumor in mice. Biochem Pharmacol 2007;73:1405–1411.
22. Yanagitani A, Yamada S, Yasui S, *et al.* Retinoic acid receptor α dominant negative form causes steatohepatitis and liver tumors in transgenic mice. Hepatology 2004;40:366–375.
23. Nakamura N, Shidoji Y, Yamada Y, *et al.* Induction of apoptosis by acyclic retinoid in the human hepatoma-derived cell line, HuH-7. Biochem Biophys Res Commun 1995;207:382–388.
24. Kada N, Suzuki T, Aizawa K, *et al.* Acyclic retinoid inhibits neointima formation through retinoic acid receptor beta-induced apoptosis. Arterioscler Thromb Vasc Biol 2007;27:1535–1541.
25. Nakajo S, Okamoto M, Masuda Y, *et al.* Geranylgeraniol causes a decrease in levels of calreticulin and tyrosine phosphorylation of a 36-kDa protein prior to the appearance of apoptotic features in HL-60 cells. Biochem Biophys Res Commun 1996;226:741–745.
26. Hashimoto K, Morishige K, Sawada K, *et al.* Geranylgeranylacetone inhibits lysophosphatidic acid-induced invasion of human ovarian carcinoma cells *in vitro*. Cancer 2005;103:1529–1536.
27. Ince N, Wands JR. The increasing incidence of hepatocellular carcinoma. N Engl J Med 1999;340:798–799.
28. Solomon C, White JH, Kremer R. Mitogen-activated protein kinase inhibits 1,25-dihydroxyvitamin D3-dependent signal transduction by phosphorylating human retinoid X receptor α. J Clin Invest 1999;103:1729–1735.
29. Liu M, Iavarone A, Freedman LP. Transcriptional activation of the human p21(WAF1/CIP1) gene by retinoic acid receptor. J Biol Chem 1996;271:31723–31728.

ARTICLE

Journal of Cellular Biochemistry 111:1035–1041 (2010)

Journal of Cellular Biochemistry

Simultaneous Color-Coded Imaging to Distinguish Cancer "Stem-Like" and Non-Stem Cells in the Same Tumor

Atsushi Suetsugu,[1,2,3] Yosuke Osawa,[3] Masahito Nagaki,[3] Hisataka Moriwaki,[3] Shigetoyo Saji,[4] Michael Bouvet,[2] and Robert M. Hoffman[1,2*]

[1] *AntiCancer, Inc., San Diego, California*

[2] *Department of Surgery, University of California, San Diego, California*

[3] *Department of Gastroenterology, Gifu University Graduate School of Medicine, Gifu, Japan*

[4] *Department of Surgical Oncology, Gifu University Graduate School of Medicine, Gifu, Japan*

ABSTRACT

In this study, we demonstrate that the differential behavior, including malignancy and chemosensitivity, of cancer stem-like and non-stem cells can be simultaneously distinguished in the same tumor in real time by color-coded imaging. CD133$^+$ Huh-7 human hepatocellular carcinoma (HCC) cells were considered as cancer stem-like cells (CSCs), and CD133$^-$ Huh-7 cells were considered as non-stem cancer cells (NSCCs). CD133$^+$ cells were isolated by magnetic bead sorting after Huh-7 cells were genetically labeled with green fluorescent protein (GFP) or red fluorescent protein (RFP). In this scheme, CD133$^+$ cells were labeled with GFP and CD133$^-$ cells were labeled with RFP. CSCs had higher proliferative potential compared to NSCCs in vitro. The same number of GFP CSCs and the RFP NSCCs were mixed and injected subcutaneously or in the spleen of nude mice. CSCs were highly tumorigenic and metastatic as well as highly resistant to chemotherapy in vivo compared to NSCCs. The ability to specifically distinguish stem-like cancer cells in vivo in real time provides a visual target for prevention of metastasis and drug resistance. J. Cell. Biochem. 111: 1035–1041, 2010.

KEY WORDS: CANCER STEM CELLS; CD133; HEPATOCELLULAR CARCINOMA; NUDE MICE; CHEMOTHERAPY; GFP; RFP; COLOR-CODED IMAGING

The cancer stem cell hypothesis of solid tumors, has thus far not been fully substantiated since stem and non-stem cells have not been simultaneously visualized and compared in real time in tumors of live animals.

There are two general models of heterogeneity of cells in solid cancers. One model is that among the heterogeneous cells in a tumor, most have only limited malignant potential, but a subset can be highly malignant and tumor initiating. This model therefore predicts that a distinct subset of cells has greater ability to form new tumors and metastasis compared to other cancer cell types in the tumor. This type of cell is termed a cancer stem cell (CSC) and the other types of cancer cells in the tumor are non-stem cancer cells (NSCC). The alternative model is that any given cell in a tumor has an equal probability and ability to form a tumor and metastasis [Bonnet and Dick, 1997; Reya et al., 2001; Al-Hajj et al., 2003; Abraham et al., 2005; Dean et al., 2005; Bao et al., 2006; Jordan et al., 2006].

Expression of the surface protein CD133 (also known as AC133 and prominin-1) is a marker that may identify CSCs in solid tumors including brain [Reya et al., 2001; Bjerkvig et al., 2005]; lung [Donnenberg et al., 2007]; melanoma [Monzani et al., 2007]; prostate [Miki et al., 2007]; kidney [Bussolati et al., 2005]; and colon [O'Brien et al., 2007; Ricci-Vitiani et al., 2007]. CD133 is also expressed in developing epithelia and differentiated cells [Jaszai et al., 2007; Mizrak et al., 2008]. CD133 was originally identified as a marker for stem and progenitor cells of the hematopoietic system [Yin et al., 1997; Toren et al., 2005]. We and others previously reported that the CD133-expressing cells play a critical role in the self-renewal of a range of hepatic stem cells [Suetsugu et al., 2006; Ma et al., 2007; Yin et al., 2007].

Our laboratory has pioneered the use of fluorescent proteins to visualize in vivo phenomena, including primary tumor growth, tumor cell motility and invasion, metastatic seeding and colonization, angiogenesis, and the interaction between the tumor and its microenvironment in live animals in real time [Chishima et al., 1997; Yang et al., 2000; Hoffman, 2005; Hoffman and Yang, 2006a,b,c]. Fluorescent proteins of different colors have now been characterized, and these can be used to color-code cancer cells of a

Grant sponsor: National Cancer Institute; Grant number: CA132971.

*Correspondence to: Robert M. Hoffman, PhD, AntiCancer, Inc., 7917 Ostrow Street, San Diego, CA 92111.
E-mail: all@anticancer.com

Received 15 July 2010; Accepted 20 July 2010 • DOI 10.1002/jcb.22792 • © 2010 Wiley-Liss, Inc.
Published online 29 July 2010 in Wiley Online Library (wileyonlinelibrary.com).

specific genotype or phenotype. For example, the interaction of highly metastatic cancer cells labeled with green fluorescent protein (GFP) and low metastatic cancer cells labeled with red fluorescent protein (RFP) can be directly compared in vivo in the same tumor [Tome et al., 2009]. Real-time imaging with fluorescent proteins is especially important when evaluating the efficacy of therapeutics on metastasis and tumor recurrence [Hoffman, 2005; Hoffman and Yang, 2006a,b,c]. A set of multicolor fluorescent proteins can be used simultaneously for multifunctional in vivo imaging. These properties make fluorescent proteins optimal for cellular imaging in vivo [Hoffman, 2005].

In the present study, we utilized real-time, color-coded imaging with fluorescent proteins for real-time imaging of the comparative behavior of CSCs and NSCCs in the same tumor including malignancy and drug sensitivity.

MATERIALS AND METHODS

CELL LINE AND CULTURE CONDITION

Huh-7, a human hepatocellular carcinoma (HCC) cell line, was obtained from the Japanese Collection of Research Bioresources (Tokyo, Japan). The cells were maintained in RPMI 1640 supplemented with 10% heat-inactivated fetal bovine serum, 1% penicillin and streptomycin. The cells were cultured at 37°C in a 5% CO_2 incubator.

GENE TRANSDUCTION OF FLUORESCENT PROTEINS TO HUH-7 CANCER CELLS

Huh-7 cells were labeled with RFP or GFP as previously reported [Bussolati et al., 2005] using retroviruses expressing GFP or RFP. Huh-7 cells were transfected with retroviruses. Clones expressing RFP or GFP were established by subculture in selective medium containing G418.

ISOLATION OF CSC FROM HUH-7 CELLS

The expression of CD133 was determined by standard flow cytometry analysis using a phycoerythrin (PE)-labeled antibody against human CD133/2 (Miltenyi Biotech, Bergisch Gladbach, Germany) with an FACS-vantage flow cytometer (Becton Dickinson, San Jose, CA). The data were analyzed using CELLQuest software (Becton Dickinson Immunocytometry Systems, San Jose, CA). Approximately 49% of Huh-7 cells expressed CD133. In this study,

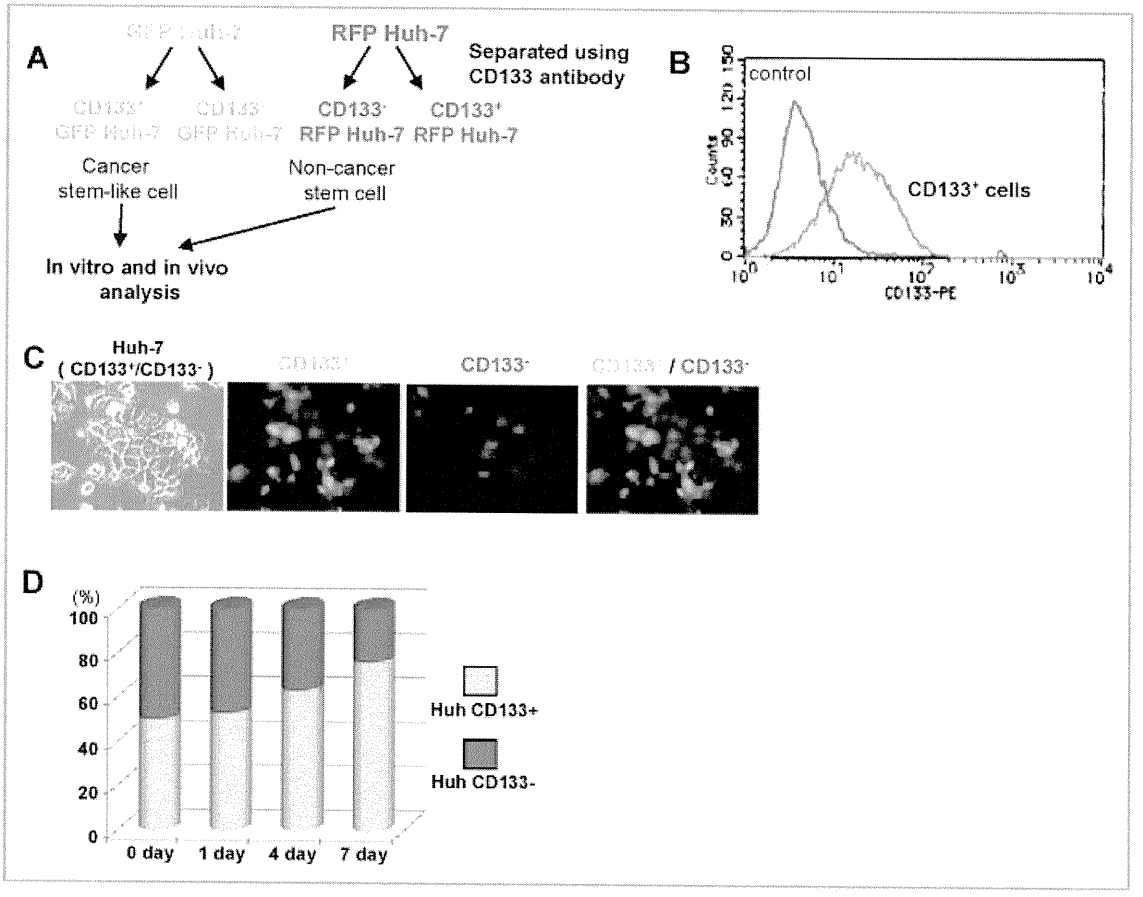

Fig. 1. A: Schematic representation of experimental protocol. $CD133^+$ cells and $CD133^-$ cells were isolated, respectively, from the established GFP and RFP Huh-7 cells by magnetic bead sorting. GFP-expressing $CD133^+$ Huh-7 cells were used as CSCs (GFP-CSCs), and RFP-expressing $CD133^-$ Huh-7 cells were used as NSCCs (RFP-NSCCs). B: CD133 expression in Huh-7 cells was examined by FACS analysis. The results shown are representative of at least three independent experiments. C: The same number of the GFP-CSCs and RFP-NSCCs were mixed and co-cultured. GFP-expressing and RFP-expressing cells were observed at 24 h after plating. D: The total intensities of GFP and RFP were compared in the wells after plating at the indicated time points. The results are representative of at least three independent experiments.

$CD133^+$ Huh-7 cells were considered as CSCs and $CD133^-$ Huh-7 cells were as NSCCs. $CD133^+$ Huh-7 cells were isolated by magnetic bead sorting using the MidiMACS system (Miltenyi Biotech) with monoclonal CD133 antibody (Miltenyi Biotech) according to the manufacturer's instructions. A schematic representation of the experimental protocol is shown in Figure 1A. The same number of the CSCs labeled with GFP and the NSCCs expressing RFP were mixed and co-cultured in dishes or co-implanted in mice.

IN VIVO IMAGING

We used color-coded in vivo imaging [Hoffman, 2005; Hoffman and Yang, 2006a,b,c] to visualize CSCs or NSCCs in vivo, using the Olympus OV100 Small Animal Imaging System (Olympus Corp., Tokyo, Japan).

The Olympus OV100 which contains an MT-20 light source (Olympus Biosystems, Planegg, Germany) and DP70 CCD camera (Olympus), was used for cellular imaging in live mice. The optics of the OV100 fluorescence imaging system have been specially developed for macroimaging as well as microimaging with high light-gathering capacity. The instrument incorporates a unique combination of high numerical aperture and long working distance. Four individually optimized objective lenses, parcentered and parfocal, provide a 10^5-fold magnification range for seamless imaging of the entire body down to the subcellular level without disturbing the animal. The OV100 has the lenses mounted on an automated turret with a high magnification range of 1.6× to 16× and a field of view ranging from 6.9 to 0.69 mm. The optics and antireflective coatings ensure optimal imaging of multiplexed fluorescent reporters in small animals. High-resolution images were captured directly on a PC (Fujitsu Siemens, Munich, Germany). Images were processed for contrast and brightness and analyzed with the use of Paint Shop Pro 8 and Cell^R (Olympus Biosystems) [Yamauchi et al., 2006].

The viable cell area was measured using National Institutes of Health (NIH) Image J analysis software program (available at http://rsb.info.nih.gov/nih-image/).

NUDE MOUSE CANCER MODELS

Nude mice were anesthetized with a ketamine mixture (10 μL ketamine HCl, 7.6 μL xylazine, 2.4 μL acepromazine maleate, and 10 μL H_2O) injected into the peritoneal cavity. To simultaneously compare CSCs and NSCCs in the same tumor, the same number of liver GFP-CSCs and RFP-NSCCs were mixed, and injected into the spleen (1×10^6 cells/50 μL matrigel) during open laparotomy or injected subcutaneously (1×10^6 cells) in non-transgenic nude mice.

All animal studies were conducted in accordance with the principles and procedures outlined in the NIH Guide for the Care and Use of Animals under assurance A3873-1. Animals were kept in a barrier facility under HEPA filtration.

CHEMOTHERAPY

Nude mice were subcutaneously implanted with GFP-CSCs and RFP-NSCCs as described above. The mice were treated in the following groups: (1) saline (vehicle/control) (intraperitoneally), (2) CDDP (10 mg/kg, intraperitoneally) (Cisplatin, Nippon Kayaku CO., Japan), (3) bevacizumab (BEV) (5 mg/kg, intraperitoneally) (Avastin, Roche, South San Francisco, CA), and (4) combined treatment with CDDP and BEV (CDDP/BEV). Control, CDDP and BEV injections were performed on a weekly basis from day 7 after tumor implantation. By this time, the HCC tumors reached approximately 20 mm. Each treatment arm involved 10 HCC-bearing mice. No significant effects on body weight, morbidity, or severe toxicities were observed in any treatment arm. Tumor growth was monitored weekly by measuring the long tumor axis and body weights were recorded. Animals were sacrificed at 6 weeks, and tumors were harvested for analysis. The

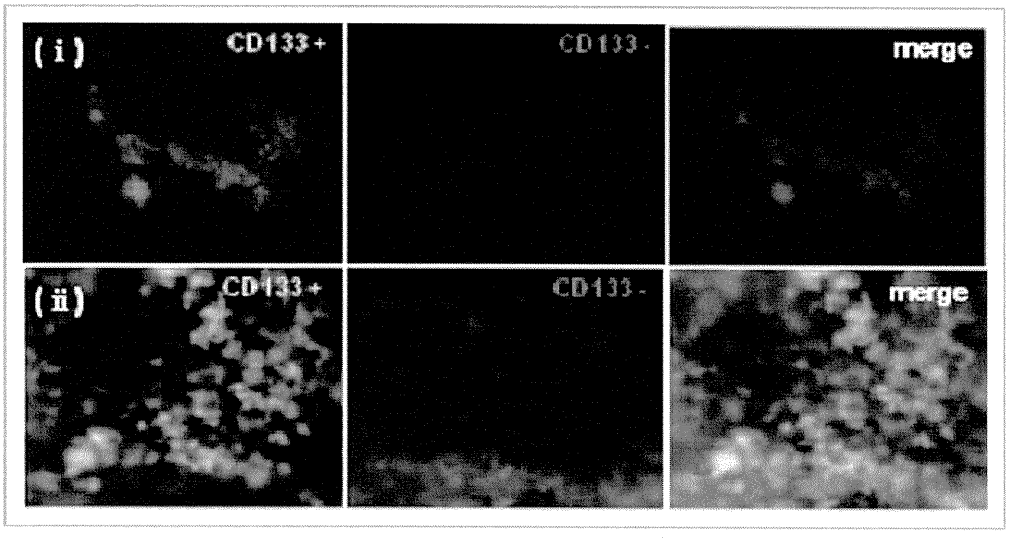

Fig. 2. A mixture of GFP-CSCs and RFP-NSCCs (1×10^6/50 μl) cells was injected into the spleen of nude mice during open laparotomy. On day 28 after cell injection, GFP and RFP fluorescence was observed in tumor colonies in the liver. (i) A diffuse metastasis and (ii) a nodular metastasis.